

THE MECHANICS OF
DRY SURFACE GRINDING

By

EARLE ROBERT MARSHALL

B.S., Massachusetts Institute of Technology

1948

Submitted in Partial Fulfillment of the

Requirements for the Degree of


MASTER OF SCIENCE

from the

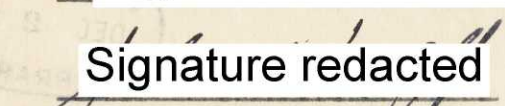
Massachusetts Institute of Technology

1949

Signature of Author
Department of Metallurgy
September 9, 1949


Signature redacted

Signature of Professor
in Charge of Research


Signature redacted

Signature of Chairman
Department Committee
on Graduate Students


Signature redacted

Metall
Thesis
1949

THE LIBRARY OF
THE MASSACHUSETTS INSTITUTE OF TECHNOLOGY

BY

LESLIE ROBERT MARSHALL

Submitted in partial fulfillment of the

1949

Requirements for the Degree of

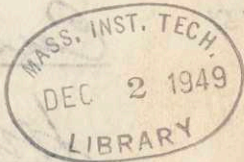
MASTERS OF SCIENCE

from the

Massachusetts Institute of Technology

1949

[Faint handwritten signatures and text, including "C. P. Marshall" and "John W. Hoff"]



Signature of Author
Department of Metallurgy
September 9, 1949

Signature of Professor
in Charge of Research

Signature of Chairman
Department Committee
on Graduate Studies

TABLE OF CONTENTS

	<u>Page Number</u>
ACKNOWLEDGMENTS	1
INTRODUCTION	2
SUMMARY	4
DISCUSSION OF PREVIOUS WORK	5
APPARATUS	
Surface Grinder	7
Force Dynamometer	7
Bridge Circuits	8
Brush Strain Recorder	8
Dynamometer Calibration	9
Vibration Damping	9
Dynamometer Stiffness	10
Diamond Dresser	11
X-ray Equipment	11
MATERIALS	
G rinding Specimens	12
Grinding Wheels	13
RESULTS	
The Work-Piece	14
Cut Standardization	15
Forces v. Table Direction	16
Dressing Technique	18
Constant Conditions	22

TABLE OF CONTENTS (Cont'd)

	<u>Page Number</u>
Forces vs. Depth of Cut	23
Forces vs. Table Speed	23
Forces vs. Wheel Speed	24
Forces vs. Work Width	24
Forces vs. Hardness	25
Ratio of Components	25
Coefficients of Friction	28
X-Ray Diffraction Studies	29
Burn	30
Elastic Effects	32
Generalized Expression of Data	34
CONCLUSIONS	40

LIST OF FIGURES

<u>Number</u>	<u>Title</u>
1	Force Dynanometer in Operation
2	Schematic Side View of Dynanometer
3	I-Beam and Vertical Ring Member
4	Dynamometer Frame
5	Vertical Bridge Circuit
6	Horizontal Bridge Circuit
7	Block Diagram of Force Recording Components
8	Brush Strain Recorder
9	Dynamometer Natural Frequencies
10	Force Decay Curves after Damping
11	Diamond Pyramid Wheel Dresser
12	Microstructure of Annealed S.A.E. 52,100
13	Microstructure of Oil-Quenched S.A.E. 52,100
14	Graph of S.A.E. 52,100 Hardness vs. Drawing Temperature
15	Brush Chart for Horizontal Work-Piece
16	Brush Chart for Vertical Work Piece
17	Graph Showing Effect of Elasticity on Grinding Cuts and Forces
18	Brush Chart Showing Forces Approaching Limiting Values
19	Graphs of Grinding Forces vs. Cut Depth
20	Graphs of Grinding Forces vs. Table Speeds
21	Graphs of Grinding Forces vs. Inverse Wheel Speeds
22	Graphs of Grinding Forces vs. Width of Work
23	Graphs of Friction Forces for Stationary Wheel vs. Ground Work-Piece
24	X-Ray Diffraction Rings for Annealed Specimen

LIST OF FIGURES (Cont'd)

- 25 Diffraction Rings for Ground Surface(Cut Depth: 0.00025 inches,
Etch Depth: 0.)
- 26 Diffraction Rings for Ground Surface(Cut Depth: 0.00025 inches,
Etch Depth: 0.00020 inches)
- 27 Diffraction Rings for Ground Surface(Cut Depth: 0.00050 inches,
Etch Depth: 0.00020 inches)
- 28 Diffraction Rings for Ground Surface(Cut Depth: 0.00050 inches,
Etch Depth: 0.00040 inches)
- 29 Diffraction Rings for Ground Surface(Cut Depth: 0.0010 inches,
Etch Depth 0.00040 inches)
- 30 Diffraction Rings for Ground Surface(Cut Depth: 0.0010 inches,
Etch Depth: 0.00060 inches)
- 31 Graph of Depth of Cold Working vs. Cut Depth
- 32 Brush Chart Showing Forces for Surface Burn
- 33 Diagram for Analysis of Elastic Effects
- 34 Generalized Plot of Grinding Data

LIST OF TABLES

<u>Number</u>		<u>Page</u>
I	Force vs. Table Motion	17
II	Dressing Technique	20
III	Pyramid Dressing (No Spark-out)	21
IV	Constant Values of Variables	22
V	Forces vs. Hardness	26
VI	Ratio Components	27
VII	Elastic Effects	39
VIII	Energy vs. Chip Size	36

ACKNOWLEDGMENTS

The author wishes to express his thanks to Professor Shaw and Professor Wulff for inspiration, encouragement and advice.

He also wishes to express his gratitude to the Timken Roller Bearing Company for having done so much to make this investigation possible. Dr. E. S. Roland as their representative has been exceptionally helpful and has given much sound and needed criticism.

The author is grateful to Dr. J. T. Norton for his helpful advice and for providing the X-ray equipment used in these experiments. Finally, the author wishes to thank Mr. Jose Morales who was a joint participator in these X-ray experiments.

INTRODUCTION

The present project for studying grinding was sponsored by the Timken Roller Bearing Company. Their purpose is to encourage experimental and theoretical investigation of the process. From knowledge so gained, it is hoped that better ground surfaces, and thus improved bearing life and performance will result.

Several research fellowships have been granted on this project. This paper is largely concerned with the mechanical variables. Another fellowship was granted for the study of residual stresses, and a third for determining the action of cutting fluids and the determination of cutting temperatures.

The idea of studying grinding forces was suggested by Dr. M.C. Shaw in whose Metal Cutting Laboratory this research was carried out. He has successfully correlated the mechanics of single point cutting with chemical and metallurgical factors, and consequently felt that this method would be equally profitable here.

In the present investigation a force dynamometer was built to measure the normal and tangential forces exerted on the work by the wheel. Force measurements were made under the simplest possible conditions in order to isolate the important factors and thus obtain as basic an understanding as possible.

For this reason, this initial study of the mechanics of grinding was confined to dry surface grinding without cross-feed. Much of the theoretical knowledge gained in this investigation would not have been possible, for example, if cross-feed had been used.

The forces determined under these conditions were then correlated with the important variables such as feeds, speeds, size and position of work, wheel dressing, sparking-out and so forth. Certain factors of considerable practical and theoretical interest were discovered and are described in the text.

SUMMARY

An electronic force dynamometer was constructed for measuring the normal and tangential forces in dry surface grinding. S.A.E. 52,100 was used as the material.

A new diamond dressing technique was studied and found to give lower and more consistent force readings. It materially reduced burning of the work.

Simple relationships were found to exist between forces and each of the following variables: cut depth; table speed; wheel speed; and work width. A method was found to connect all these variables for a given wheel. This relationship may be significant in studying the strength of metals.

The ratio of tangential to normal components was only slightly higher than the friction coefficient. During burning it was lower.

Grinding forces were nearly the same for 43 and 65 Rockwell C.

X-ray diffraction studies indicated that the ground surface was cold-worked to a depth of about one half the cut that produced it.

The effect of elasticity in the grinding system was studied. Mathematical equations were derived to show the relationship between down-feed and the actual amount removed. Another was derived to explain sparking-out. They were checked experimentally.

The study was carried out on Alundum and Silicon Carbide wheels. The latter gave higher forces and burned the work more readily.

DISCUSSION OF PREVIOUS WORK

A study of the literature has not revealed any previous work reported on the direct measurement of forces in grinding, although there are numerous papers covering force measurements in other machining operations (planing, turning, drilling, etc.). One of the first of such direct studies of machining forces was conducted by Afanassiew*1(Russia) in 1885. He used hydraulic pressure measurements to analyze the forces in chip formation. Since that time, the literature has been full of descriptions of mechanical and electrical force dynamometers.

Until recently most of such studies of the mechanics of machining operations were empirical in nature and not backed up by competent theoretical analysis. The first such analysis was published by Vaino Piispanen*2 (Finland) in 1937. He analyzed the stresses and strains in the chip in terms of cutting forces. This was followed by similar work of M.E. Merchant*3 in this country in 1944 and 1945.

A series of studies on cylindrical grinding has been published by Boston*4 Energy input to the grinding machine was correlated with such

-
- *1 Afanassien, "Determination of work and Pressure in the Formation of Chips ",
Tech. Bulletin, Institute in Petersburg, p. 84, (1885.)
- *2 Piispanen, Vaino. Teknillinen Aikakanslenti, 27, 315-322 (1937)
- *3 Merchant, M.E., J.A. Mechanics, 11, A168-A175 (1944)
J. Applied Physics, 16, p. 267 (1945)
J. Applied Physics, 16, p. 318 (1947)
- *4 Boston, O.W. et al, Trans. of A.S.M.E., Nov. 1947, Vol. 69, No. 2, p.125
Trans. of A.S.M.E., Nov. 1947, Vol. 69, No. 8, p. 891
Trans. of A.S.M.E., Feb. 1948, Vol. 70, No. 8, p. 893

factors as wheel wear, surface finish and cutting fluids. Results on this type of machine are not easily compared with the present investigation.

X-ray diffraction studies were correlated in this report with mechanical features. Wulff*1 made a somewhat similar study by electron diffraction, of the depth of cold worked material in ^{ground} 18-8 stainless steel. He found evidence of severe distortion to a depth of 6×10^{-4} centimeters. Values of the same order of magnitude were found in this paper.

The only other reference found to diffraction studies on grinding was that published recently by Glikman and Stepanov*2 (Russia). Residual stresses measured by X-ray diffraction were shown to vary from 18 kilograms per square millimeter to 0 over a depth of one millimeter. No study was made of the cold working introduced.

The mechanical features accompanying burning can be interestingly compared with work of L.P. Tarasov*3 on injury in ground surfaces. A correlation of the etching techniques he has developed for detecting injury in ground surfaces with our force measurements, is planned for the near future.

*1 Wulff, John, Am. Inst. of M. & M. Eng., Vol. 145, 1941, p. 295

*2 Glikman, L.A. and Stepanov, F.A., Journal of Technical Physics, Vol. 16 No. 7, 1946, pp. 791-802

*3 Tarasov, L.P., Trans. of A.S.M., Vol. 36, 1946, p. 389

APPARATUS

Surface Grinder

A Norton 6-18 surface grinder was used for all grinding experiments. In order to study the effect of wheel speed a special d.c. shunt motor was installed. Spindle speed was adjusted over the range of 2200 to 3500 revolutions per minute by means of adjustable field rheostats. Wheel speed was measured with an "Ideal" electric tachometer. A hydraulically operated table provided uniform table speeds over the range of 2 to 16 feet per minute. A stop watch was used to determine table speed.

Force Dynamometer

An electronic dynamometer was constructed for the purpose of measuring the forces exerted by the wheel on the work-piece. Figure 1 shows the apparatus in operation mounted on the table of the surface grinder.

Figure 2 is a schematic side view of the dynamometer. The work-pieces are held in vices fixed to the top of an aluminum I-beam. The I-beam is supported by four circular springs. These rings are in turn supported by two long horizontal bars. This member of the apparatus is shown separately in Figure 3. The vertical component of the grinding force is measured by noting the strain in the four rings. Electric resistance strain gages are attached to each ring to determine the strain.

The long bars under the vertical strain rings rest on two shafts that are mounted in four ball bearing pillow blocks bolted to a base frame. The frame is shown separately in Figure 4 secured to the grinder table.

The I-beam structure is restrained from rolling horizontally on the shafts by a long wire which is attached to the frame at the ends

and the I-beam near the middle. Another force measuring ring with electric strain gages is mounted on this wire. The strain in this ring is measured to determine the horizontal component of the grinding force. The friction in the bearings is negligible when compared with the horizontal force. The horizontal ring is made independent of vertical loads by making the wire so long that the angle through which it moves due to vertical deflection of the system will induce negligible force in the wire and ring.

Bridge Circuits

There are two strain gages on each vertical ring. These gages are connected to form the arms of a Wheatstone bridge. The vertical bridge circuit and wiring plan are shown in Figure 5. The gages are so arranged in the bridge circuit that the vertical force reading is independent of any torque effect. Torques produced by an eccentric position of the grinding wheel (due to table traverse or cross feed), or by the horizontal component, are thus cancelled out. The gage arrangement also compensates for temperature changes.

There are four electric strain gages on the horizontal ring to provide maximum sensitivity and temperature compensation. They are connected as shown in Figure 6.

Brush Strain Recorder

Each bridge output was amplified by an individual Brush Strain Analyzer (BL-3105). The Analyzer outputs were used to drive a Brush double pen oscillograph (BL-202). This recorded the force readings graphically as a function of time. There were three chart speeds: 5, 25, and 125

millimeters per second. A Block diagram of the force recording components is shown in Figure 7. Figure 8 is a photograph of the three Brush units. With this set-up, considerably greater sensitivity was available than required. For example, at maximum amplification, one millimeter pen deflection corresponded to 0.02 pounds horizontal load, and 0.05 pounds vertical.

The frequency response of this system is flat over the range 0 to 100 cycles per second.

Dynamometer Calibration

Vertical calibration was accomplished by loading the dynamometer with 5-pound dead weights and noting the pen deflection. Output was linear through 50 pounds load. The usual calibration adjustment was 10 millimeters for 5 pounds.

Horizontal calibration was similarly carried out by loading with a spring scale (push gage) through 10 pounds. Usual calibration was 10 millimeters for 2 pounds. Output was linear. The spring scale was easily checked by comparing its reading with that of the dead weights on the vertical set-up.

Both circuits were checked for calibration before and after each run.

Vibration Damping

The natural frequency of the dynamometer in the vertical direction was determined by plucking and observing the resulting pattern on the Brush recorder. It was 83 cycles per second. The horizontal frequency was similarly determined as 17 cycles per second. (Figure 9)

Spindle speeds used corresponded to 38 to 58 cycles per second. No serious resonant phenomenon was encountered over this range.

However, after initial test runs it was found that even slight unavoidable wheel unbalance was sufficient to cause force variations of up to 5 per cent. The resulting broad pen lines made accurate force readings impossible. Consequently, a dashpot was installed. SAE 120 oil was the damping fluid. The piston was attached to the I-beam (Figures 2 and 3) while the surrounding cylinder was bolted to the grinding table (Figures 2 and 4). Figure 10 shows the force decay curves after introduction of the dashpot. The time constant for the horizontal system (time for the force to drop to 36.8 per cent) is now 0.10 seconds while for the vertical it is 0.06 seconds. Vibrations no longer interfere with force readings.

Dynamometer Stiffness

The vertical stiffness of the grinding machine-dynamometer-wheel system was easily measured by pressing the stopped wheel down against the work. The total spring constant, K , was then determined by dividing the increment of force by the increment of downfeed (since the curve was linear). K was thus found equal to 6,790 pounds per inch, with any wheel used in these tests.

The vertical spring constant, K_d , of the dynamometer alone was determined by loading the dynamometer and observing deflection between the work and the table. It was 11,920 pounds per inch.

The stiffness, or spring constant of the grinding machine without the dynamometer is then easily calculated as follows:

$$\frac{1}{K_g} = \frac{1}{K} - \frac{1}{K_d} = \frac{1}{6,790} - \frac{1}{11,920}$$

$K_g = 15,800$ pounds per inch

Thus introduction of the dynamometer reduced the total stiffness from 15,800 to 6,790 or slightly more than one half. The effect of the stiffness on the grinding properties is considered experimentally and theoretically below.

Diamond Dresser

A special wheel dressing diamond* in the form of an eight sided pyramid was obtained in order to bring the wheels to a standard condition before testing. Figure 11 shows how the flat on a face of the diamond is held tangent to the wheel. Each time a wheel is dressed, a new face is turned into position. Thus although wear on the diamond occurs, the geometry of the pyramid is maintained.

A second diamond dresser with a natural cleavage point up, was also obtained. A third similar diamond, but worn from continual use, was borrowed from the M.I.T. Machine Tool Laboratory.

X-Ray Equipment

A back reflection X-ray camera with cobalt radiation and Machlett tube was used for X-Ray diffraction studies. It was operated under the following conditions: 45 Kilivolts, 10 milliamperes, with 11-minute exposures.

* The use of this type of diamond was suggested by Dr. L.P. Tarasov of the Norton Grinding Wheel Company.

MATERIALS

Grinding Test Specimens

All grinding work-pieces were made of S.A.E. 52,100 chrome carbon bearing steel supplied by the Steel Division of the Timken Roller Bearing Company. Five-eighth-inch square bars in 10-foot lengths were received in the hot-rolled, spheroidized-annealed condition. Their analysis for Heat Number 22849 is:

	C	Mn	P _{Max.}	S _{Max.}	Si	Cr
S.A.E. 52,100 Specification	0.95 - 1.10	0.25 - 0.45	0.025	0.025	0.20-0.30	1.30-1.60
Heat 22849	1.00	.35	.016	.013	.28	1.44

In order to eliminate surface decarburization, these bars were reduced to 1/2 inch square section by planing. They were then cut to three-inch lengths for heat treatment. The 1/2-inch square section permitted oil quenching to Martensitic structure throughout.

The majority of the grinding test work was done on annealed 52,100. This was obtained by holding the specimens at 1550 degrees Fahrenheit for one hour followed by furnace cooling. The specimens were placed in cast iron chips to prevent further decarburization. The resulting hardness was 43 Rockwell "C". The microstructure is shown in Figure 12.

Specimens of higher hardness were obtained by holding in a lead pot at 1550°F. for one hour followed by quenching in oil. The hardness obtained was 65 Rockwell "C", and the microstructure is shown in Figure 13.

Tempered specimens were obtained by holding the quenched bars one hour in a circulating air furnace. The hardnesses

obtained are shown in Figure 14 for the following drawing temperatures:

70° F. (as quenched)
200° F.
400° F.
600° F.
800° F.

Hardnesses were uniform across the sections.

Grinding Wheels

Four 8-inch diameter, 3/4 inch wide grinding wheels were used in these tests. They were manufactured by the Norton Grinding Wheel Company under the following designations.

32A36-H8VBE	32A60-H8VBE
32A46-H8VBE	37C36-J-V

The first three had aluminum oxide abrasive (32 Alundum), but differed in grain size (36, 46, and 60 openings per inch in the sizing screen). They were medium low strength bond (H), had fairly high grain spacing (8), and were vitreous bonded (VBE). These wheels are widely used for surface grinding hard steels.

The fourth wheel had Silicon Carbide abrasive (37C), size 36 grain, medium strength bond (J), and was vitreous bonded (V). It is generally used for materials of low tensile strength and was selected for these tests in order to get a very different cutting action characteristic of this abrasive.

These wheels are generally operated at a maximum speed of 2900 revolutions per minute. The 3/4 inch widths always overlapped the 1/2 inch (or less) wide work-piece.

RESULTS

The Work-Piece

Annealed S.A.E. 52,100 was used for all tests except where the grinding forces for various hardnesses were investigated. The 3 x 1/2 inch square heat-treated specimen was tried in two grinding positions. First, the 3-inch length was placed horizontally along the direction of table motion. In all tests the 3/4-inch wide wheel overlapped the work width, and there was no cross-feed. The force patterns obtained are shown in Figure 15. The steadily increasing forces made it difficult to determine a force to select as representative of the test conditions.

However, when the same test specimen was held with the three-inch length vertical, the forces approached a definite limit. (Figure 16) The asymptotic appearance is a result of the retarding effect of the dash-pot.

The steadily increasing forces of the horizontal specimen were caused by the advancing heat wave generated during the deformation accompanying grinding. During the longer horizontal cut, the heat was able to get ahead of the wheel. In this case, the specimen extended 0.375 inches above the vice jaws. An average rise in temperature of 200 degrees Fahrenheit, for example, would cause an increase in specimen height of about 0.0005 inches. Thus a cut depth of 0.0005 inches could easily be doubled under these conditions.

In the vertical specimen, however, the whole specimen tends to expand rather than part of it. Moreover, much less material is removed from the side for the same cut. Thus, less heat energy is obtained for the same volume, and the temperature rise is lower. Finally the specimen is

contacted over a greater portion of its length by the cooler vice.

Consequently, the vertical specimen was adopted for all tests, and expansion was only of importance during very heavy cuts. As a further control, cuts were equally spaced (two seconds apart) so that the specimen would tend to expand a definite amount prior to each equal cut.

Cut Depth Standardization

If the wheel is brought level with the work, and then the wheel is fed down and a cut taken, the depth removed will be some fraction of the downfeed. This is because the vertical force exerted during grinding pushes the work away from the wheel slightly due to elasticity in the grinding system.

If an additional equal downfeed is applied on a second cut, the wheel now faces this feed plus the amount remaining from the first cut. The wheel removes a similar part of this total and the second depth removed is larger than the first. When this process is continued, the depth removed per cut is found experimentally to approach the actual downfeed as a limit.

Figure 17 and Table VII show how this happened in another case. (Test details on the figure). The depth removed per cut was determined by measuring the original specimen height and the height after each cut (with a hand micrometer). The curves through the experimental points are theoretical and will be derived below.

Simultaneous recording of the two force components shows that they likewise approach a definite limit when the depth removed per cut very nearly equals the downfeed (Figure 17). Hereafter, the forces recorded

for a given depth of cut (and specified conditions) were determined by making equal downfeeds and watching the Brush Chart until the forces reached these limits. Five or ten subsequent readings were then averaged to obtain the forces characteristic of this cut. A sample Brush chart is given in Figure 18. These superimposed cuts may not give the same forces as those obtained from grinding off a given depth from unground material, since previous cuts have altered the surface, by working and introducing stresses, etc. However, it is the only feasible method of obtaining any quantity of data. Moreover, it corresponds to industrial grinding practice.

Forces vs. Table Direction

The table can carry the work-piece in the direction of wheel surface motion, or against it. In industrial practice the former is known as "downhill", and the latter as "uphill" grinding.

In the following test, the tangential and normal grinding forces were investigated for the two table directions. Ten successive force readings were taken at a cut depth of 0.00075 inches, the wheel being lifted out of the way on the return stroke of the table. Ten cuts were similarly taken for the opposite direction. The test conditions and the forces obtained are shown on Table I.

No difference in force within the precision of measurements could be associated with the difference in table direction for either the tangential or normal component.

The results appear logical since the speed of the work relative to the wheel is not changed appreciably by reversing the table motion. In this test, the wheel surface speed was 6280 feet per minute compared to

TABLE I

TANGENTIAL, T, AND NORMAL, N, GRINDING FORCES FOR TABLE MOTION
WITH AND AGAINST WHEEL SURFACE MOTION

Test Conditions:

Work: Annealed 52,100; 1/2 x 1/2 inch surface; dry.

Wheel: 32 A 46-H8VBE at 3000 rpm.

Cut Depth: 0.00075 inches

Table Speed: 4 feet per minute

Results:

<u>With Wheel</u>		<u>Against Wheel</u>	
T Lb.	N Lb.	T Lb.	N Lb.
2.8	5.4	2.6	5.2
2.5	5.3	2.6	5.1
2.6	5.2	2.5	5.2
2.5	5.6	2.4	5.2
2.6	5.3	2.6	5.4
2.6	5.4	2.6	5.4
2.5	5.3	2.5	5.1
2.4	5.2	2.6	5.2
2.6	5.1	2.6	5.2
<u>2.7</u>	<u>5.5</u>	<u>2.5</u>	<u>5.4</u>
Average	2.6 5.3	2.6	5.2
Per Cent Average Devi- ation.	3 2	2	2

4 feet per minute for the table. Thus the relative speeds differed by 0.13 per cent.

In all tests below, forces were obtained without regard to table direction. No appreciable force difference was observed in these tests due to this cause.

Dressing Technique

Grinding wheels are dressed in order to sharpen the grit particles in a wheel which has become dull or glazed due to use. Dressing also removes metal particles which become embedded in (or "load") the wheel.

Diamond dressing was studied because of its importance in obtaining reproducible data. Its effect on grinding forces and on the work-piece was observed in the following tests. Three techniques were studied.

In the first method, the special diamond pyramid dresser was used. (See Apparatus and Figure 11). To dress the wheel, the diamond was passed back and forth axially across the wheel surface. At each pass, 0.0005 inch was removed until the wheel was clean of loading, (2 to 4 times). Further passes without downfeed were then made, until no further wheel grits were removed ("spark-out").

A test of twenty grinding cuts of 0.001 inch each was then made on an annealed work-piece. The test conditions and the average forces recorded are given on Table II. The wheel was then redressed and the test repeated (ten times altogether). A new face on the diamond was turned into position for each dressing.

In the second method, a commonly used industrial technique was tried. The wheel was dressed with a sharp new diamond, the natural cleavage

point held upwards directly under the wheel (instead of tangentially at an angle of 15° as with the pyramid). The wheel material was otherwise removed in a similar fashion to the first method. A similar set of ten tests of twenty cuts each was conducted (Table II).

In the third method, the second was repeated but with a diamond worn dull from shop usage.

Each force value on Table II is an average of values for any test between dressings of the wheel. Forces were reproducible to within 2 to 3 per cent average deviation for a given dressing of the wheel, regardless of the dressing technique. However, from one dressing to another the forces varied more widely.

Table II shows that burning of the work surface occurred in several of the tests. The conditions accompanying burning are considered under a separate heading below.

The results on Table II show that:

1. The average forces are lower for the diamond pyramid.
2. The deviations of the pyramid forces from one dressing to another, were about $1/2$ that for the sharp diamond and $1/5$ that for the dull diamond.
3. The work surface did not burn on any diamond pyramid test, but did burn on most of the other tests. It burned after the fewest cuts on the dull diamond.

Diamond pyramid dressing without spark-out, and for various amounts of wheel material removed per pass was also tried. Table III gives the results for the same test conditions as Table II. One test of twenty cuts was made for each dressing.

TABLE II

DIAMOND DRESSING TECHNIQUE

Work: Annealed 52,100; 1/2 x 1/2 inch surface, dry.

Wheel: 32A60-H8VBE, 8 x 3/4 inch at 3000 rpm.

Table Speed: 4 feet per minute (no cross-feed)

Cut Depth: 0.001 inches.

Forces: Normal, N, and Tangential, T, in Pounds.

Test Number	Diamond Pyramid			Sharp Regular Diamond			Dull Diamond		
	T	N	Remarks	T	N	Remarks	T	N	Remarks
1	2.9	5.3	--	4.0	7.5	Burn, 16 cuts	4.3	6.8	Burn, 16 cuts
2	3.0	5.2	--	3.5	6.5	Burn, 18 cuts	2.9	5.0	----
3	2.9	5.6	--	3.4	6.3	----	--	---	Burn, 1 cut
4	2.8	5.0	--	2.9	5.3	----	--	---	Burn, 1 cut
5	2.9	5.2	--	3.1	5.7	Burn, 20 cuts	3.0	5.2	----
6	2.7	5.0	--	3.2	6.3	Burn, 20 cuts	4.2	7.5	Burn, 7 cuts
7	3.2	5.5	--	3.5	7.1	----	4.7	8.2	Burn, 3 cuts
8	3.1	5.4	--	3.4	6.9	Burn, 16 cuts	2.9	5.0	Burn, 17 cuts
9	2.8	4.5	--	3.7	7.2	Burn, 13 cuts	2.6	4.5	----
10	3.1	5.3	--	4.0	8.0	Burn, 8 cuts	3.3	6.4	Burn, 11 cuts
Average	2.9	5.2		3.5	6.7	Burn 7 of 10 tests	3.5	6.1	Burn 7 of 10 tests
% Average Deviation	+ 4	+ 4		+ 8	+ 10		+ 20	+ 19	*(Two omitted from average)
% Maximum Deviation	10	13		17	21		43	43	

TABLE III
PYRAMID DRESSING NO SPARK-OUT

<u>Dressing</u>	<u>T</u> Lb.	<u>N</u> Lb.
0.00100 inch 2 cuts	2.7	4.9
0.0005 inch 4 cuts	2.6	4.9
0.00025 inch 8 cuts	2.6	5.0

Thus without spark-out, the forces appear to be slightly lower than with it. This may be because dressing is somewhat rougher in the former, giving sharper cutting edges.

The pyramid dressing operations for the tests on Tables II and III were conducted on a recently cut diamond. These tests do not show one important advantage of this diamond. This is its tendency to maintain its geometry with continued wear because of the tangential position of its faces when dressing.

Consequently, the ten pyramid tests on Table II were repeated after several hundred dressing operations. The average tangential force was now 2.7 pounds \pm 9 per cent average deviation with a maximum of 15 per cent. For the normal force the corresponding values were: 5.0 \pm 8 per cent with 14 maximum. Still no burning was experienced. Thus, although the force scatter went up, the pyramid still gave better results than the sharp regular diamond.

The pyramid dressing with spark-out was conducted on all the

following tests. When studying the effect of a grinding variable such as cut depth on the forces, the wheel was dressed and then the whole test run without redressing. As shown above, this permitted greater reproducibility than if dressing interceded. The forces were checked for the same cutting conditions before and after each run to insure that constant wheel condition had been maintained.

Constant Conditions

The effect of certain important grinding variables on the forces were studied by changing one and holding the others constant. To do this a set of constant conditions was adopted as follows:

TABLE IV
VARIABLES AND THEIR VALUES WHEN HELD CONSTANT

<u>Variable</u>	<u>Value When Constant</u>	<u>Range When Independent Variable</u>	<u>Units</u>
Cut Depth	0.00075 for Alundum Wheels	0.000125	Inches
	0.00025 for Silicon Carbide Wheels	to 0.003	
Table Speed	4	2 to 16	Feet Per Minute
Wheel Speed	3000	2250 to 3500	Revolutions Per Minute
Width	0.5	0.140 to 0.5	Inches
Hardness	43 (Annealed)	43 to 65	Rockwell "C"

Each variable was studied for the three Alundum and the Silicon Carbide wheels (See Materials).

More general methods of expressing the variables when they are simultaneously changed were then developed.

Forces vs. Depth of Cut

Figure 19 shows graphically the variation of the normal and tangential forces with cut depth. There is a separate graph for each of the four wheels. The Alundum wheels are arranged in the order of decreasing grain size (36, 46, 60), followed by the Silicon Carbide wheel. Each point represents the average of ten force readings. The forces were determined at cut increments of 0.000125 inch up to 0.001 inch and in 0.0005 inch thereafter until the surface burned.

For lower depths of cut, the force components were proportional to the cut depth. A marked transition occurred, however, where the forces increased less rapidly. This transition occurred at between 0.00075 and 0.001 inch on the Alundum wheels, and at 0.000375 inch for the Silicon Carbide.

The forces for the three Alundum wheels were similar for the same cut. The Silicon Carbide wheel gave forces about twice as great.

Burning of the surface occurred at smaller depths of cut for smaller grain size on the Alundum wheels, but the Silicon Carbide wheel caused burning at even lower cuts.

Forces vs. Table Speed

Figure 20 gives the variation of forces with table speed for the same four wheels. The table speeds were 2, 3, 4, 6, 8, 10, 12 and 16 feet per minute.

At table speeds over 6 feet per minute the error due to time lag of the dashpot was greater than 1 per cent. The forces were corrected by making a semi-logarithmic correction curve based on the time constants of Figure 10. The corrections were checked experimentally by running an exceptionally well-balanced wheel with and without the dashpot.

The shapes of the curves remarkably resemble those of Figure 19. The forces increase in proportion to the table speed when the speed is low. At higher speeds, the forces increase less rapidly. Transitions occurred at 4 to 8 feet per minute table speed for each wheel.

The Alundum wheel forces were again similar. The forces for the Silicon Carbide wheel were only slightly lower for the same table speed although the cut was one third that for the Alundum wheels.

Forces vs. Wheel Speed

Tests indicate that the force components are inversely proportional to wheel speed over the range studied, i.e. 2250 to 3500 revolutions per minute. To show this the forces are plotted against the inverse of the wheel speed on Figure 21. Inverse proportionality is then indicated by the fact that straight lines drawn through the points can be extrapolated through the origin.

Forces vs. Work Width

To run this test, four annealed specimens of widths 0.140, 0.259, 0.338 and 0.497 inches were mounted in the vices so that the wheel passed over one after the other. The grinding wheel thus presented the same cutting action to each specimen for the same depth of cut.

In addition to the usual constant cut depths of 0.00075 and 0.00025 inch for the Alundum and Silicon Carbide wheels, cuts of 0.0015 and 0.0010 inch, respectively, were investigated. This was done to see how work width affected the forces in both the proportional and non-proportional parts of Figure 19.

The results are shown on Figure 22. In every case the normal and the tangential components were proportional to the work width.

Forces vs. Hardness

Table V gives the test conditions, and the hardnesses of the specimens tested. Because so little variation of forces with hardness was obtained, only three of the seven different heat treatments were investigated.

Test specimens were mounted as in the work width experiment so that the wheel passed successively over each specimen. Each force value is an average of ten cuts.

The normal forces did not appear to be affected by the change in hardness (heat treatment). The tangential forces appear to be slightly lower for the quenched specimen than for the annealed on the Alundum wheels. But the differences are on the border of statistical significance.

Ratio of the Tangential, T, to the Normal Component, N.

Thus far, the tangential and normal components were treated as separate entities. Their ratios in the previous tests will now be considered.

In the tests of cut depth and table speed, the two force components were proportional to these independent variables near the origin. (Figures 19 and 20). In the tests on wheel speed and work width, the force curves were

TABLE V

NORMAL, N, AND TANGENTIAL, T, GRINDING FORCES FOR S.A.E.

52,100 WORK-PIECES HEAT TREATED TO THREE HARDNESSES

Work: S.A.E. 52,100, 1/2 x 1/2 inch surface, dry
(See Heat Treatment below)

Table Speed: 4 feet per minute

Wheels: 3000 rpm. for 8 x 3/4 inch
(Specified below)

Cut Depth Inches	Wheel Grain Size	Wheel Grit	43 Rockwell C Annealed		52 Rockwell C Tempered 800° F.		65 Rockwell C As Quenched	
			T Lb.	N Lb.	T Lb.	N Lb.	T Lb.	N Lb.
.00075	36	Alundum	2.3	5.0	2.3	5.0	2.2	5.1
.00075	46	"	2.3	4.9	2.3	5.0	2.1	4.9
.00075	60	"	2.5	5.4	2.3	5.5	2.2	5.5
.00025	36	Silicon Carbide	1.8	4.0	1.7	4.1	1.8	4.1

straight lines extending from the origin. (Figures 21 and 22). In these cases the ratios of the components are easily obtained by taking the ratio of the slopes. The results are as follows:

TABLE VI
RATIO OF T/N FOR SPECIFIED TESTS ON FOUR WHEELS

Test	36, Alundum (32A36-H8VBE)	46, Alundum (32A46-H8VBE)	60, Alundum (32A60-H8VBE)	36, SiC (37C36JV)
Cut Depth (Low Cuts)	.52	.48	.57	.50
Table Speed (Low Speed)	.51	.49	.51	.45
Wheel Speed	.68	.58	.55	.46
Width	.56	.52	.46	.48
Average	.57	.52	.52	.47
Max. Deviation in Per Cent	19	12	12	6

The values for any wheel have considerable spread. This variation could not be associated with the magnitude of either force component. The values for the Alundum wheels were similar with the size 36 grain somewhat higher. The silicon carbide ratios are slightly lower.

The values in the upper portions of Figures 19 and 20 (not shown) tended to decrease slightly, but not in every case. The scatter increased somewhat.

One reason for the large scatter is that each test involved a different dressing condition of the wheel. The maximum deviation for each force component

was about 10 per cent. (Table II), for pyramid dressing. But the maximum deviation here is nearly twice this. The whole error can be accounted for if it is assumed that the experimental error for each component is independent. If the components are divided, the new relative error is statistically nearly the sum of the two relative errors, or approximately 20 per cent. This is close to the maximum of 19 per cent here.

Coefficient of Friction of Wheel on Work-Piece

The horizontal and vertical friction forces were easily determined holding the wheel stationary and forcing the wheel down on the work at low table speed. Different interferences provided different downward forces because of elasticity in the grinding system. The test had the advantage of maintaining the same geometry of wheel to work as during grinding.

The resulting horizontal and vertical friction forces were recorded as usual by the dynamometer on the Brush chart. Values so obtained are plotted on Figure 23. The wheel was recently dressed and the work-piece ground on this wheel immediately prior to the test. The data were reproducible from one dressing to another, in contrast to the previous test.

The coefficients of friction are equal to the slopes of these curves. The values decrease for decreasing grain size on the Alundum wheels. The Silicon Carbide value is intermediate.

Only in the case of the Silicon Carbide wheel was the ratio of grinding components (Table VI) as low as the friction coefficient. And this was the wheel giving the highest forces for a given cut. This suggests that when the cutting forces are high, a greater element of friction rather than cutting action is present.

X-Ray Study of Cold Working in the Work-Piece

Cold working of a polycrystalline material causes broadening of diffracted x-ray lines. When cobalt radiation was used with a back reflection camera, two rings of nearly the same diameter ($K\alpha$ doublet) were reflected from the α -Iron 310 plane. When the rings broadened from cold working the doublet became unresolved. Consequently, this condition gave a convenient qualitative dividing line between cold worked and lesser worked material. The "depth of cold working", as used below, is thus defined as the region where this doublet is just resolvable to the eye.

The test specimens used were the usual 1/2 inch square annealed S.A.E. 52,100 bars. Three different depths of cut were investigated: 0.00025, 0.00050, and 0.0010 inches. Each specimen was ground by taking ten successive cuts of one of these depths. The grinding test conditions were the same as for the cut depth test (Figure 19). The grinding wheel was number 32A46-H8VBE.

The X-ray beam was directed perpendicularly against the ground surface. The specimen to film distance was 5.79 cm. This gave a 310 α_1 ring approximately 3.85 cm. in diameter when reflected from the A-Ferrite in the annealed material.

Figure 24 is a diffraction photograph of an annealed unworked specimen. The two outer rings are from a Tungsten reference powder used for investigation of residual stresses (not reported here, see Introduction). The next two rings are the resolved α_1 and α_2 310 rings. Only a cross-shaped part of the rings are photographed (for convenience in stress determinations).

Cold working was studied as a function of depth by removing successive layers of 0.0002 inches with a 10 per cent Nitric acid etch. Thickness measurements were made with a one-inch micrometer. Accuracy was increased

by etching both the ground and the opposite surface (similarly ground). The total decrease in thickness was thus twice that for one surface. (0.0004 inches).

Photographs were taken of the ground surface after each removal by etching. Figures 25 and 26 show that the depth of cold working for the 0.00025 inch cut was between 0 and 0.0002 inches (since the ~~A~~ doublet was faintly resolvable at the latter etch depth). Figures 27 and 28 give similar photographs for the 0.0005 inch cut; while Figures 29 and 30 are for the 0.001 inch cut.

At etch depths of 0.0002 inches greater than required for initial resolution, the rings were easily distinguishable (not shown).

Figure 31 is a graph of the results. The depth of cold working is approximately proportional to the cut. It is roughly one half the cut that produced it. By Figure 19 the depth of cut is proportional to the force components, for slightly below 0.001 inch cut. Thus, the depth of cold working is also roughly proportional to the grinding forces.

Burn

Grinding burn is easily detected by the formation of an oxide film on the surface. The accompanying metallurgical changes in the work-piece have been studied by several techniques (See Previous Work). Here, the mechanical phenomena accompanying burning were investigated.

Figure 32 shows the force patterns on a Brush chart as burning occurred. The data on the chart is part of the tests investigating dressing technique. (Table II, Test 8, "sharp" diamond)

Burn occurred after 16 cuts of 0.001 inch. After initial appearance of burn, the tangential force increased slowly. The normal force rose rapidly and no new equilibrium was reached. The wheel became loaded with grit where

it passed over burned spots. The above sequence always occurred where burn was observed.

Rising normal forces resulted from increasing interference between wheel and work. This indicated that the wheel was cutting a smaller and smaller fraction of the downfeed.

Prior to burning the ratio of tangential to normal forces was 0.49. After burning had occurred on seven successive downfeeds this ratio had dropped to 0.32. This value was well below the friction coefficient of 0.42 for this wheel (Figure 23). If grinding during burning is frictional in nature, the lower ratio might be explained by a change in surface condition of the wheel due to glazing, or by the formation of an easy shearing layer of oxide film on the surface. This will bear further investigation.

On Figure 19 high depths of cut were associated with burning. An explanation may lie in the fact that the cutting grits became clogged with chips at high cuts. The wheel became "loaded". Metallic friction between wheel and work ensued and burning followed. This theory is further verified by the fact that the smaller grained Alundum wheels burned first.

That high cuts relative to grain size were not the only factor leading to burn is also shown by Figure 19. The 36 grit silicon carbide wheel burned at the lowest cut, and the 36 grit Alundum at the highest. Grit material is important.

Another important factor concerned with burning is the dressing technique, as was shown on Table II. The method of dressing probably effects the sharpness and hence the cutting action of the wheel grits.

Elastic Effects in Grinding

Elasticity has been found of significance in several ways. It was experimentally demonstrated that the wheel did not take a cut equal to the downfeed on the first pass. The downward cutting force pushed the work-piece away from the wheel against spring in the grinding system. Several cuts were needed to equalize downfeed and cut. (Figure 17).

If additional cuts were then made without downfeed, the work was forced closer to the wheel with each pass by the same elastic forces. The material that had not been cut in the early downfeeds above was now removed. ("Sparked-out")

In the coefficient of friction studies the wheel was made to interfere with the work so that vertical forces were obtained.

Finally in burning, the amount of cut per downfeed became smaller as burning progressed. Consequently, most of the downfeed became interference and the normal force increased rapidly.

The cut depths and forces after a certain number of downfeeds can be predicted analytically as follows:

Let N = the normal component

T = the tangential component

$U_g = T/N$ (assumed constant)

n = the number of downfeeds (equal)

f = the downfeed

d = the cut depth

x = the deflection between work and wheel

k = the spring constant between work and wheel.

By Hook's Law

$$N = kx \quad (1)$$

Restrict the derivation to the case where the forces are proportional to the cut depth, and define a cutting constant c as:

$$N = cd \quad (2)$$

Referring to Figure 33 for the first cut

$$f_1 = d_1 + x_1 \quad (3)$$

From (1), (2) and (3) is obtained

$$\frac{d_1}{f} = \frac{1}{1 + \frac{c}{k}} \quad (4)$$

On the second cut the wheel faces the deflection from the first plus the second feed. It cuts this minus the deflection during the second cut.

Thus:

$$d_2 = f + x_1 - x_2 \quad (5)$$

Substituting (1) and (2) in (5)

$$d_2 = f + \frac{c}{k} d_1 - \frac{c}{k} d_2 \quad (6)$$

Substituting (4) in (6)

$$\frac{d_2}{f} = \frac{1}{(1 + \frac{c}{k})} + \left(\frac{c}{k}\right) \frac{1}{(1 + \frac{c}{k})} \quad (7)$$

By a similar procedure to steps (5) to (7)

$$\frac{d_3}{f} = \frac{1}{(1 + \frac{c}{k})} + \left(\frac{c}{k}\right) \frac{1}{(1 + \frac{c}{k})^2} + \left(\frac{c}{k}\right)^2 \frac{1}{(1 + \frac{c}{k})^3} \quad (8)$$

By induction from (4), (7) and (8)

$$\frac{d_n}{f} = \sum_{i=1}^n \left(\frac{c}{k}\right)^{i-1} \cdot \left\{ \frac{1}{1 + \frac{c}{k}} \right\}^i \quad (9)$$

This converges for all real $\frac{c}{K}$. Here the value of N is maximum for $dn = f$, and similarly for T, (since $T/N = \text{constant}$). Therefore

$$\frac{dn}{f} = \frac{Nn}{N_{\max.}} = \frac{Tn}{T_{\max.}} \quad (10)$$

The curves through the experimental points on Figure 17 were determined from (9) and (10). (See Table VII.)

By a similar method of proof the decay of cut depth and forces can be calculated during spark-out. For the p^{th} pass the resulting expression is:

$$\frac{d_p}{d_1} = \frac{T_p}{T_1} = \frac{N_p}{N_1} = \frac{1}{(1 + \frac{K}{c})^{p-1}} \quad (11)$$

Equations (9) and (11) show that if the normal force is low for a given cut (small c), equilibrium values are reached quickly in standardizing cut, and the wheel sparks out quickly.

Generalized Expression of Data

In tests just described the effect of certain important mechanical variables on the forces was observed. Each was studied separately by holding the others constant. The tangential force component, for example, was found inversely proportional to the wheel speed and directly proportional to the work width, to the depth of cut, and to the table speed (if high values of the last two are excluded).

For these conditions the data can be neatly correlated in one simple equation. This is the expression for the energy per unit volume of chip removed:

$$\frac{E}{V} = \frac{(2 r T n)}{(vwd)}$$

Where: $\frac{E}{V}$ is the energy per unit volume of chip removed

- r is the constant wheel radius
 T is the tangential component
 n is the wheel speed
 v is the table speed
 d is the cut depth
 w is the work width

The numerator on the right gives the power output of the wheel, the denominator gives the volume of chip removed per unit time. If E/V is assumed constant, then the above test conditions are fulfilled. For example, if all variables are held constant except w and T , the latter are seen to be proportional.

The energy given up by the spindle was developed in the form of deformation and friction in the chip, work and wheel. The wheel is porous and the amount removed is usually small compared to the chip. X-ray studies on the work-piece indicate a shallow cold-worked region of one half the volume of the chip. Therefore, it seems very likely that a large part of the deformation energy is utilized in formation of the highly distorted and broken chip material.

However, when the magnitude of the energy per unit volume was calculated, it was surprisingly large. The value for the Alundum wheels was about 128×10^6 inch-pounds per cubic inch, while for the Silicon Carbide, it was 28×10^6 . For comparison, the energy involved in a simple tension test on steel is on the order of a few 100,000 inch-pounds per cubic inch.

Two factors may account for this large energy. One is the immense speed of deformation. The surface speed of the wheel is some 6000 feet per minute. Another is the small size of the chip. Some unburned chips were

obtained by grinding in a neutral atmosphere. Microscopic examination showed the chips to be on the order of a ten-thousandth of an inch in diameter.

A comparison with single point metal cutting tests indicated that as the chip size decreased, the energy per unit volume went up. The following tests illustrate this:*1

TABLE VIII

SINGLE POINT METAL CUTTING, CUT DEPTH VS.
ENERGY PER UNIT VOLUME OF CHIP REMOVED

Work Width: 0.25 inches; Tool: 18-4-1 High Speed Steel; Rake Angle: 15°;
Clearance Angle: 5°

Cut Depth	2	3	5	10	15	25	Thousandths Inch
Metal							Inch Lbs. per cubic Inch
18-8 Stainless	860,000	780,000	676,000	524,000	489,000	510,000	
Armco Iron	740,000	645,000	568,000	458,000	400,000	384,000	"

The energy per unit volume obtained on grinding chips appears to be a highly extrapolated version of the above trend. This is especially so since the chip is cut in two and three dimensions, while the single point cutting data above gives a reduction in only one dimension.

This change of deformation energy* with size bears a striking resemblance to the experiments of Griffiths*2 on glass wire. The strength of freshly formed glass fibers increased toward theoretical strength as the wire was reduced in size. Griffiths proposed a crack theory to explain these observations. More modern interpretation is based on dislocation spacing. Regardless of what theoretical explanation is eventually evolved, experimental

*1 Shaw, M.C., Mass. Inst. of Tech., Personal Communication

*2 Griffith, A.A., Phil.Trans.Royal Soc., ser.A, 1920, vol. 221, p.163

Griffith, A. A., Proc. First Internat. Congr. Appl. Mech.Delft, 1924, p. 55

evidence indicates increase toward theoretical cohesive strength with reduction in size.

The above single point data was obtained at cutting speeds of only 0.417 feet per minute, roughly $\frac{1}{15,000}$ that for our grinding data. Increase in deformation rate is also an important factor in increasing strength.

Both small size and very high speed give a clue as to why the deformation energy is so high. The reason for constancy of energy per chip volume is another question. A possible answer is that the grinding conditions are more drastic than those required to develop maximum deformation energy in the chip material. The variables d , v , n and T in the last equation would then be forced to adjust themselves to maintain this constant value of E/V . Variations from one test to another could be explained by variations in the disposition of a lesser part of this energy to the work-piece and wheel.

Constancy of E/V was not found for high cuts and table speeds. Figures 19 and 20 show that the forces drop below proportionality under these conditions. This is equivalent to a drop in E/V . A possible explanation was just recently found. In Figure 34, E/V is plotted against the power output of the wheel. ^(32A46-HBVBE) The points are for random specified grinding cutting conditions to check the general nature of the diagram. The points are seen to fall on a smooth curve.

Figure 34 suggests a physical explanation. At low energy input per unit time (power), E/V is constant, but at higher values it drops off. By Fourier's heat flow equation, the rate of development of heat determines temperature rise.

Most of the deformation energy appears as heat. A good part of this goes into the work-piece. When the energy input is very high, the strength of the material ahead of the wheel is reduced by temperature rise, and the energy required to deform it is thereby reduced. Thus the curve falls off at high power input.

The reason why this falling off is produced by high d or v is as follows. If d or v (or both) is high, for constant E/V the numerator of the last equation must also go up. But the numerator is the power output. If the power goes up, so does the temperature and E/V is thereby reduced.

Increase in width, w , does not produce this effect since the increase in power is accompanied by an increased heat sink due to the wider work piece. The temperature is thus kept from rising. Similarly, increased n is accompanied by decreased T . The power is constant and so is E/V .

There was not sufficient time to check this type of plot on all wheels and further work will have to be done to verify this completely.

ELASTIC EFFECTS IN GRINDING

Rise to Limiting Value and Successive Downfeeds, $f = 0.0075$ Inches

$$\frac{d_n}{f} = \frac{T_n}{T_{max.}} = \frac{N_n}{N_{max.}} = \sum_1^n \left(\frac{c}{k}\right)^{n-1} \left(\frac{1}{1 + \frac{c}{k}}\right)^n$$

No. of Feeds n	Experimental Values				Theoretical Values		
	T Lb.	N Lb.	d Inches	$\frac{dn}{f}$	T_n Lb.	N_n Lb.	d_n Inches
1	1.3	2.8	.0003	.490	1.28	2.63	.00037
2	2.2	4.5	.0006	.742	1.93	4.00	.00052
3	2.4	4.7	.0007	.874	2.38	4.68	.00066
4	2.5	5.2	.0007	.933	2.43	5.00	.00071
5	2.6	5.1	.0008	.967	2.51	5.18	.00073
6	2.6	5.4	.0007	.972	2.53	5.20	.00073
7	2.6	5.2	.0008	.981	2.55	5.25	.00074
8	2.5	5.2	.0007	.986	2.57	5.29	.00074
9	2.6	5.3	.0008	.989	2.58	5.30	.00074
10	2.6	5.4	.0007	.992	2.58	5.31	.00074

$T_{max.} = 2.6$ $N_{max.} = 5.35$ (Average of 9 and 10)

Logarithmic Decay in Spark-Out (No Downfeed)

$$\frac{d_n}{d_1} = \frac{T_p}{T_1} = \frac{N_p}{N_1} = \frac{1}{\left(1 + \frac{k}{c}\right)^{p-1}} \quad d_1 = 0.0075; T_1 = T_{max.}; N_1 = N_{max.}$$

No. of Passes	T	N	d	$\frac{d_p}{d_1}$	T_p	N_p	d_p
11	1.3	2.7	.0004	.512	1.33	2.74	.00038
12	0.5	1.3	.0002	.262	0.68	1.40	.00020
13	0.3	0.7	.0001	.135	0.35	0.72	.00010
14	0.2	0.4	.0000	.069	0.18	0.37	.00005

* For Plot and Test Conditions See Figure 17
For Meaning of Symbols See "Elastic Effects"

CONCLUSIONS

1. In order to investigate forces in dry grinding it was necessary to use a work-piece of short length in order to prevent the work from expanding thermally ahead of the wheel thus increasing the effective depth of cut.

2. No difference was found between forces for table motion with the wheel surface motion, or against it.

3. It was found that after a certain number of equal downfeeds that the depth of cut nearly equalled the downfeed. This method was used to get forces for a certain depth of cut. (Standardization of cut)

4. Dressing technique tests showed that the diamond pyramid dresser was superior to the usual dresser as follows:

- a. Lower forces resulted.
- b. More consistent results were obtained.
- c. Burning occurred less easily
- d. It gave more consistent results over a longer period of use.

5. The forces were found inversely proportional to the wheel speed, and proportional to the width; to the cut and to the table speed, if high values of the latter two were excluded.

6. The ratio of the tangential force to the normal force was about 0.52 for the Alundum wheels and about 0.48 for the Silicon Carbide wheels.

7. The coefficient of friction for the wheel vs. work-piece was about 0.45. It decreased slightly with grit size.

8. The coefficient of friction was lower than the tangential normal force ratio except during burn.

9. The hardness of the work did not appreciably effect the grinding forces.

10. Burning was caused by several factors as follows:

- a. Poor dressing technique.
- b. High cuts.
- c. Improper wheel grit for the work.

11. X-Ray diffraction studies showed the depth of cold working to increase proportionally with cut and forces. The cold worked layer was about half the cut that produced it.

12. The elasticity in the grinding system causes the depth of cut to fall short of the downfeed except after several continued passes. It also causes the wheel to "spark-out" for continued passes without downfeed, once a cut has been taken. These factors were expressed mathematically and checked experimentally. The wheel will give a cut more nearly to the downfeed if the forces are low. It will also "spark-out" more quickly.

13. The variables under (3) above can be connected by the equation for the energy per unit volume of chip, E/V , equal to a constant. (Excluding high cuts and table speed.)

14. There are indications that most of the energy goes into the chip. It seems likely that the energy is very high because of very large wheel speeds and the small size of the chip which tends to increase the strength of the material.

15. The E/V of (13) above falls off at high power from the wheel. This may be because the work-piece is softened by temperature rise. (This last point will have to be checked with further data.)

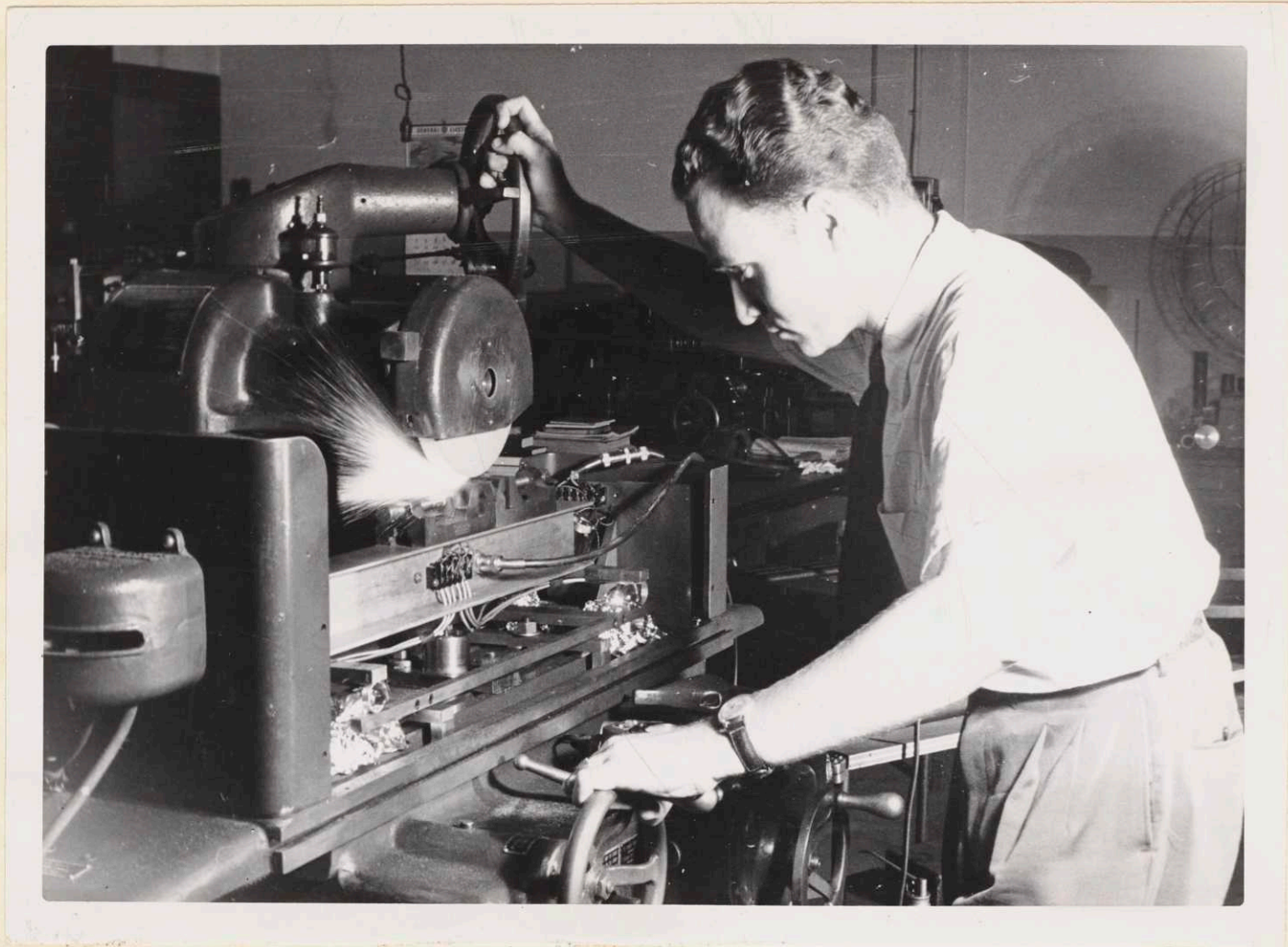


FIGURE 1

FORCE DYNAMOMETER IN OPERATION

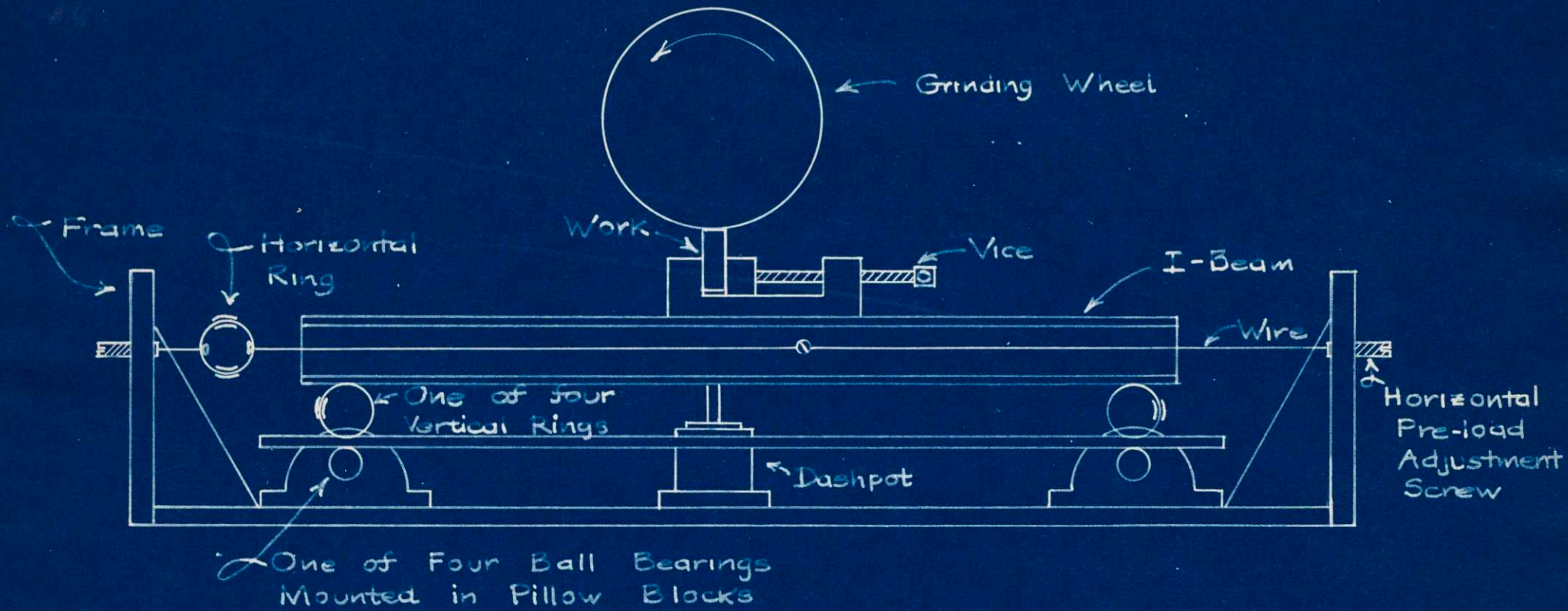


FIGURE 2
 GRINDING FORCE
 DYNAMOMETER

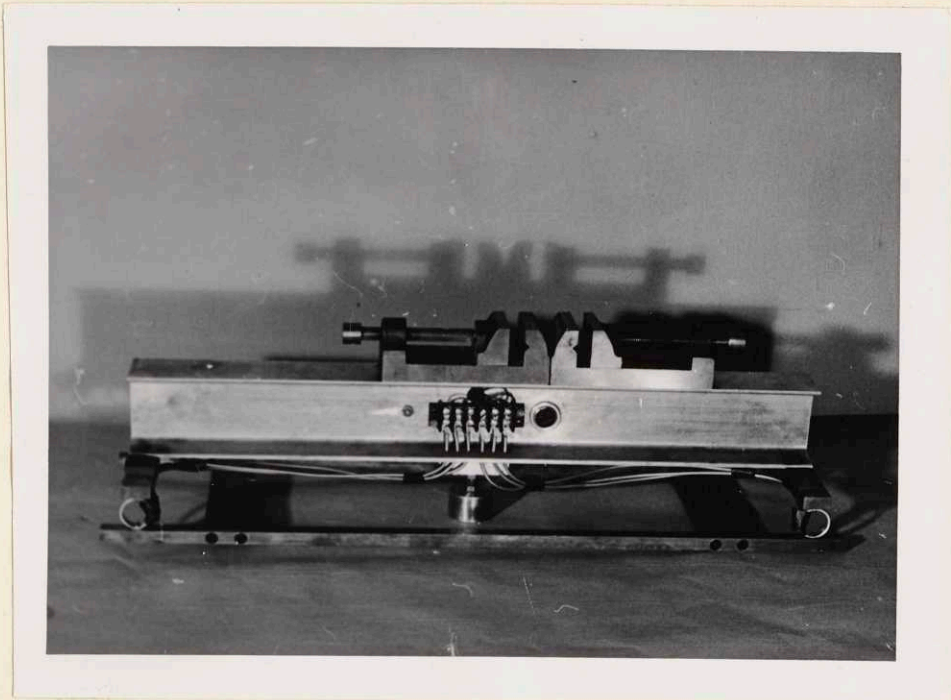


FIGURE 3

I-BEAM AND VERTICAL RING MEMBER

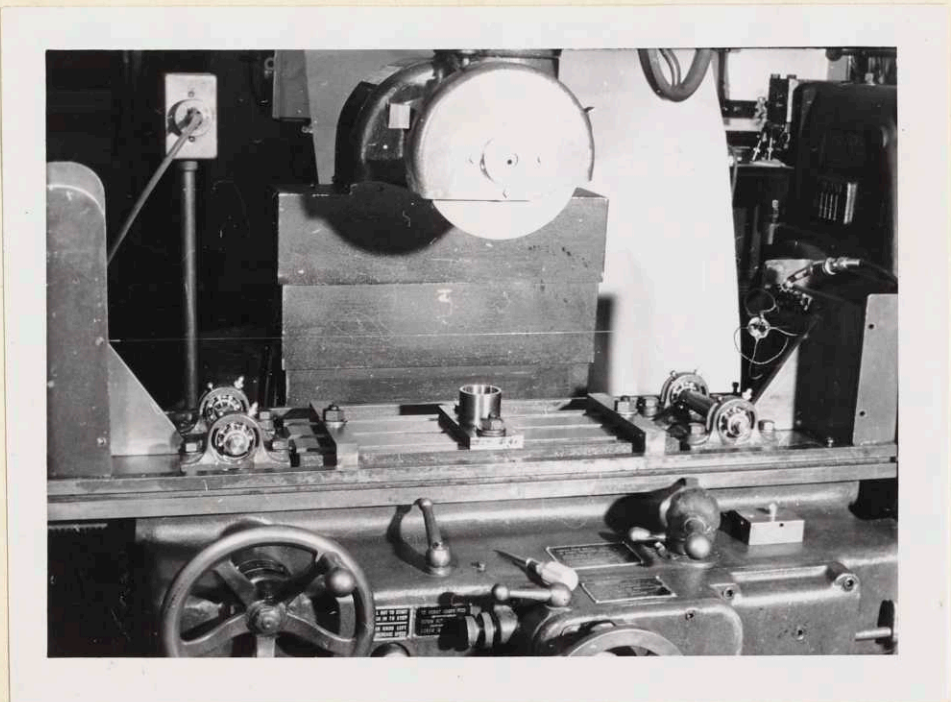
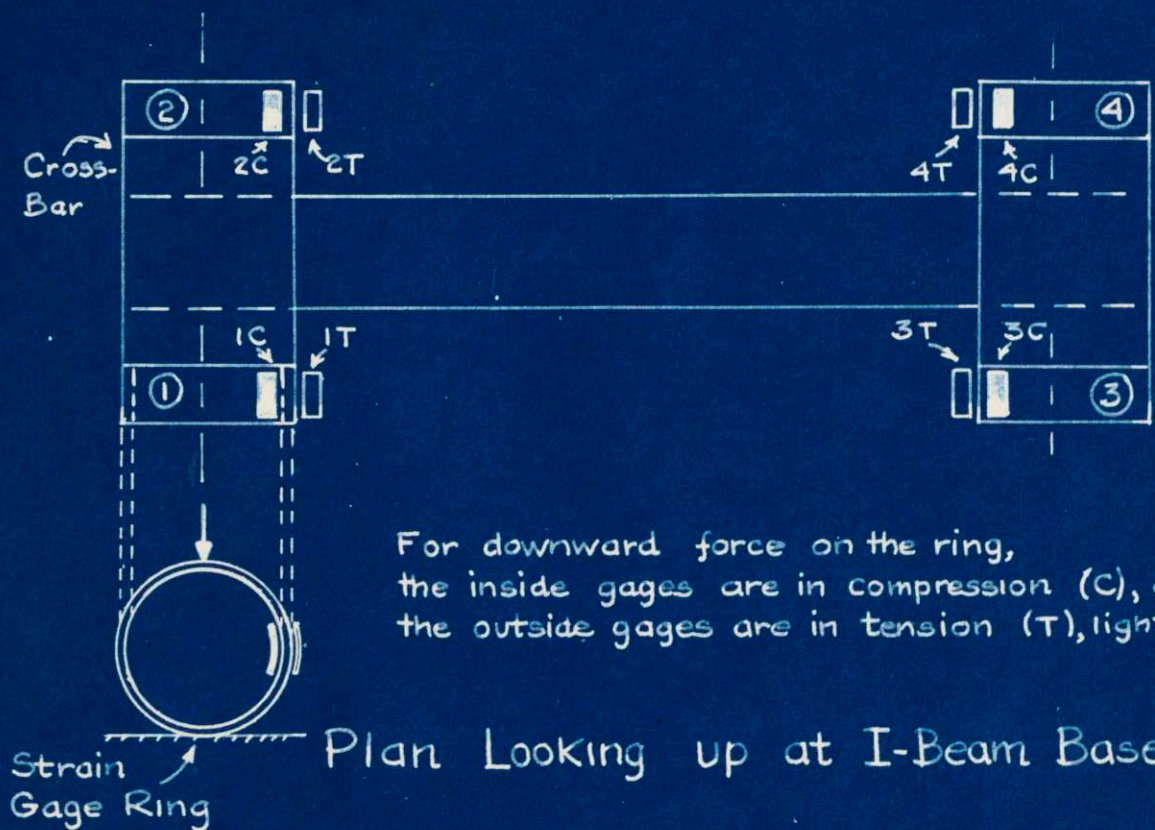
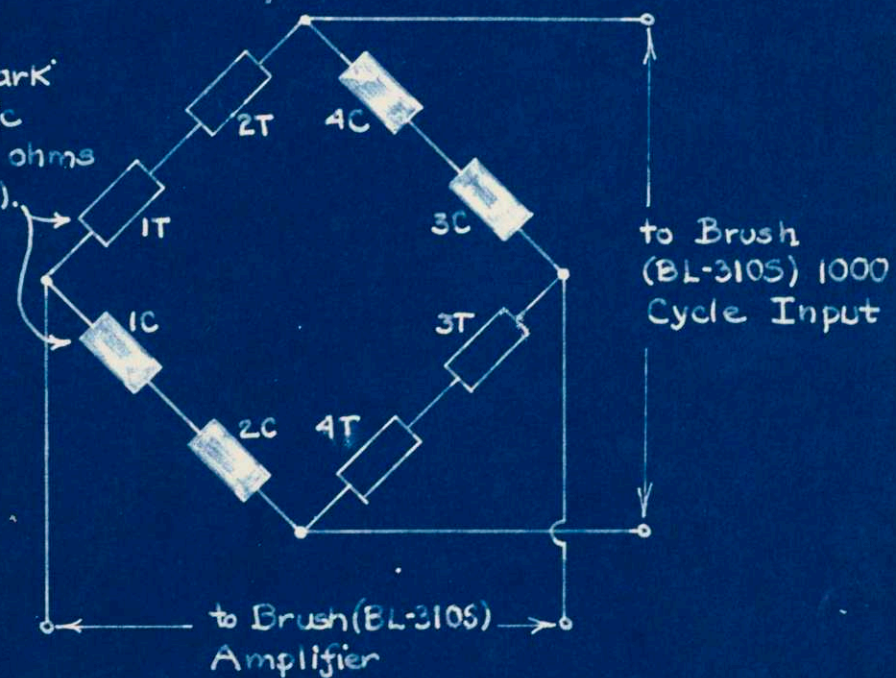


FIGURE 4

DYNAMOMETER FRAME

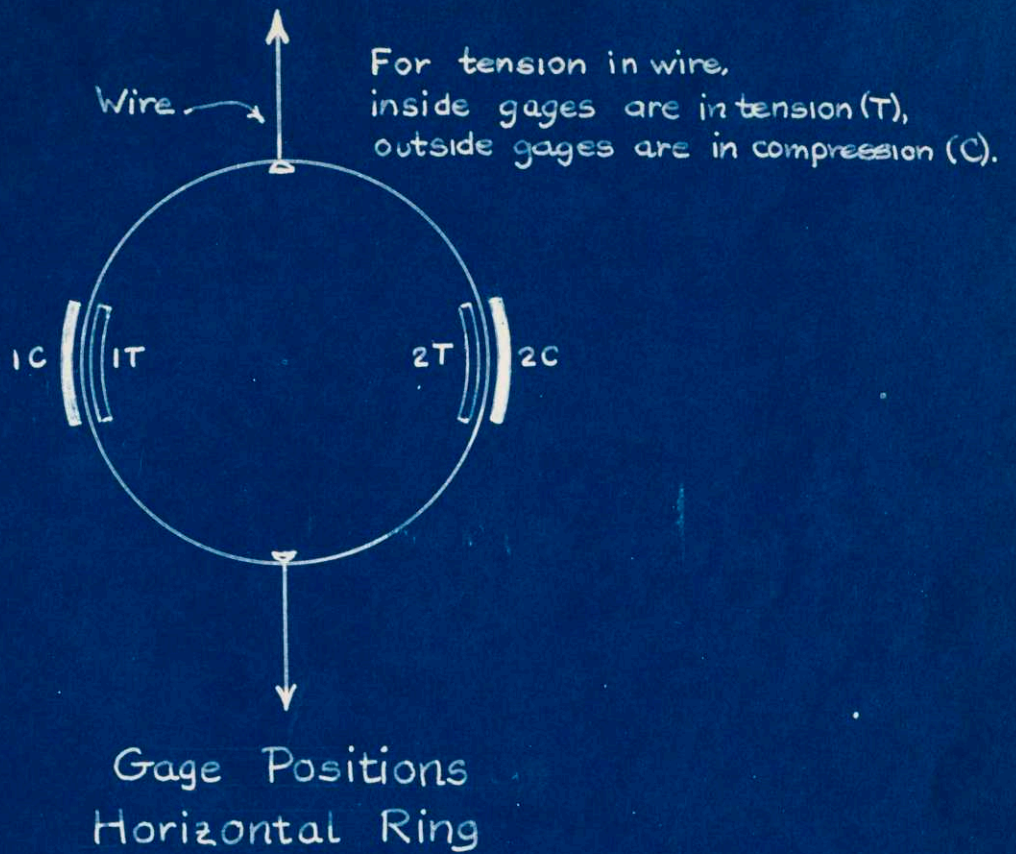


Baldwin Southwark
C-11 S-R-4 Electric
Strain Gages (300 ohms
3.05 gage factor).

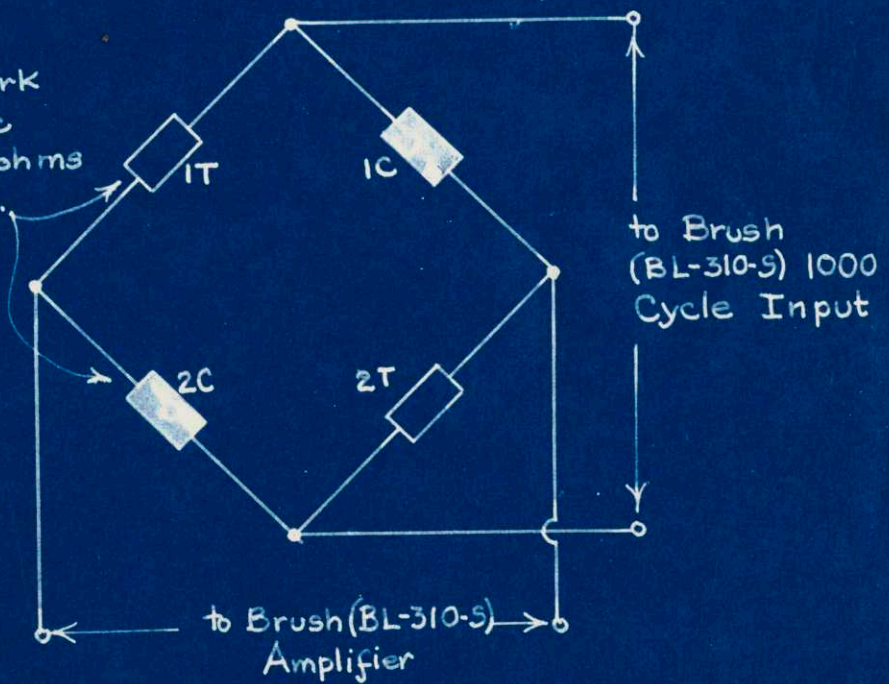


Wiring Diagram

FIGURE 5. VERTICAL BRIDGE CIRCUIT.



Baldwin Southwark
C-11 S-R-4 Electric
Strain Gages (500 ohms
3.65 gage factor).



Wiring Diagram

FIGURE 6. HORIZONTAL BRIDGE CIRCUIT.

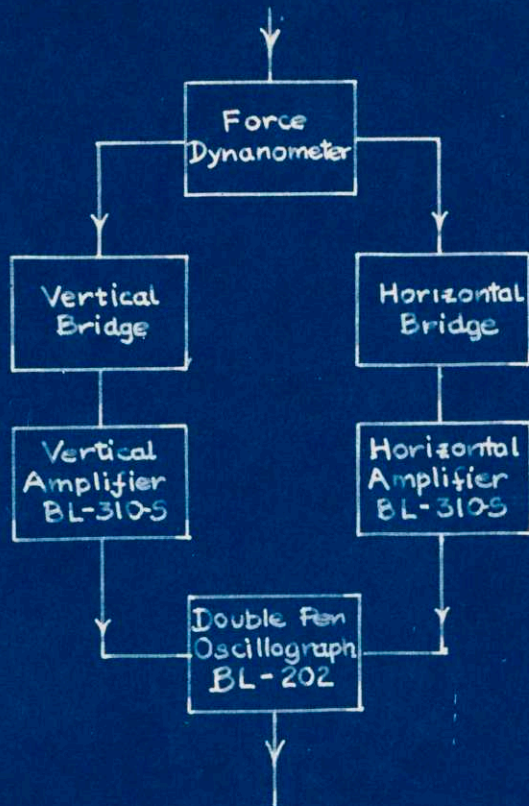


FIGURE 7
BLOCK DIAGRAM OF FORCE RECORDING COMPONENTS

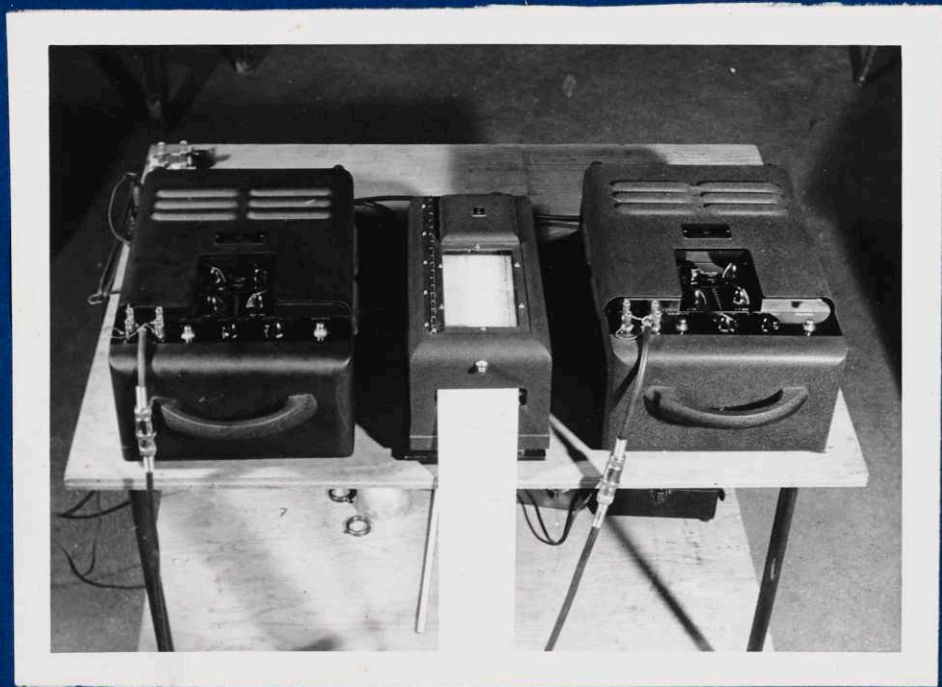
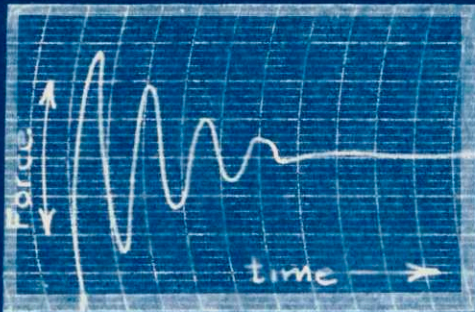
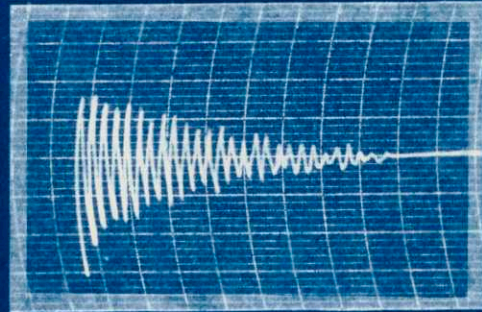


FIGURE 8
BRUSH STRAIN RECORDER

All Chart Speeds = 125 mm. per Second



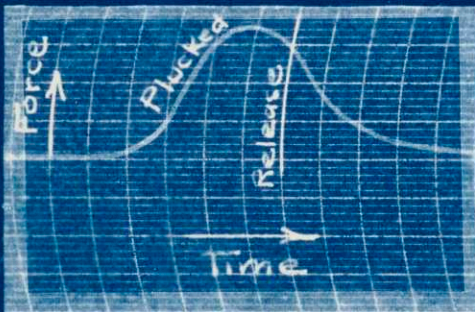
Horizontal
17 Cycles/Second



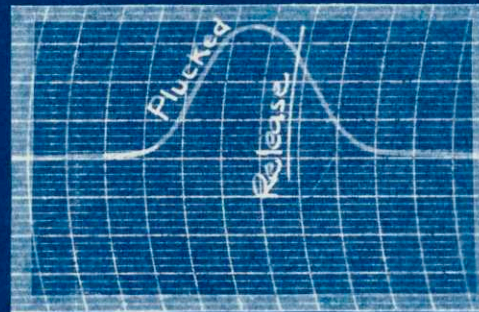
Vertical
83 Cycles/Second

(No Dashpot)

DYNAMOMETER NATURAL FREQUENCIES FIGURE 9.



Horizontal
Time Constant = .1 sec



Vertical
Time Constant = .06 sec

FORCE DECAY CURVES AFTER DAMPING FIGURE 10.

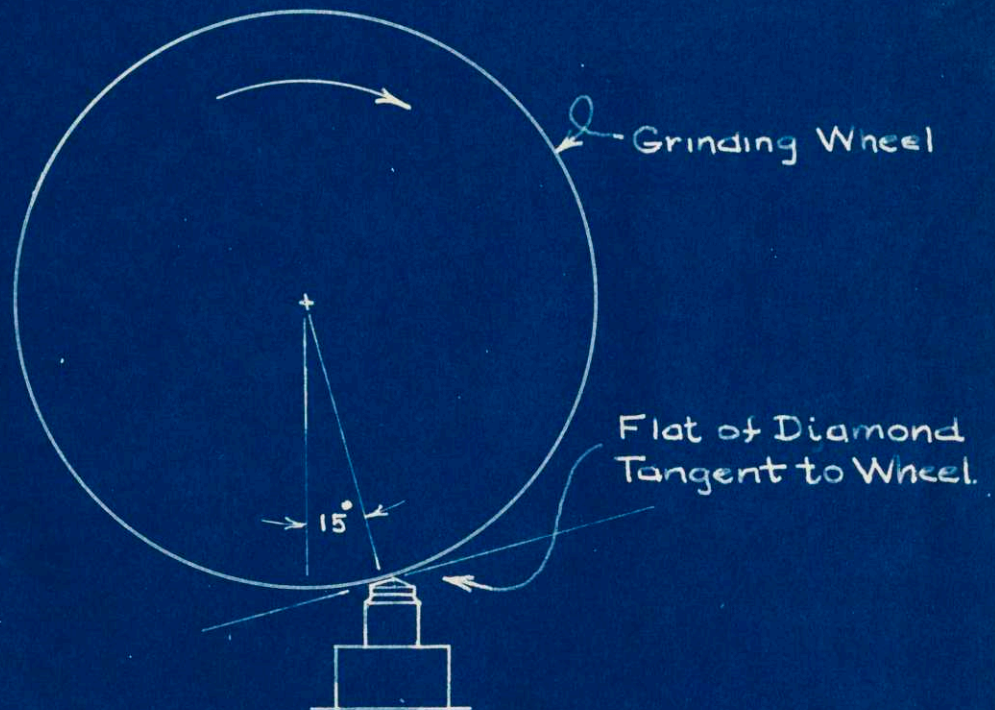
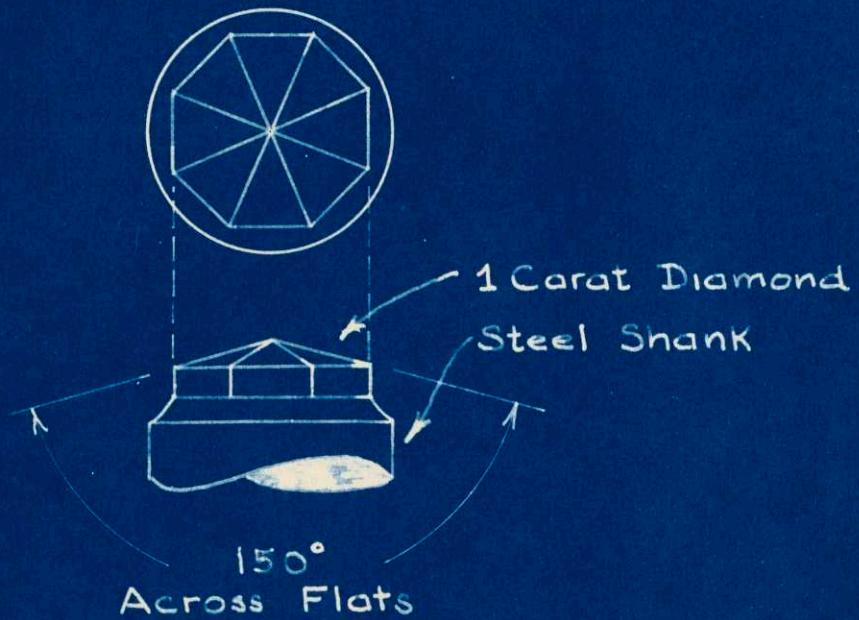


FIGURE 11
DIAMOND PYRAMID WHEEL DRESSER

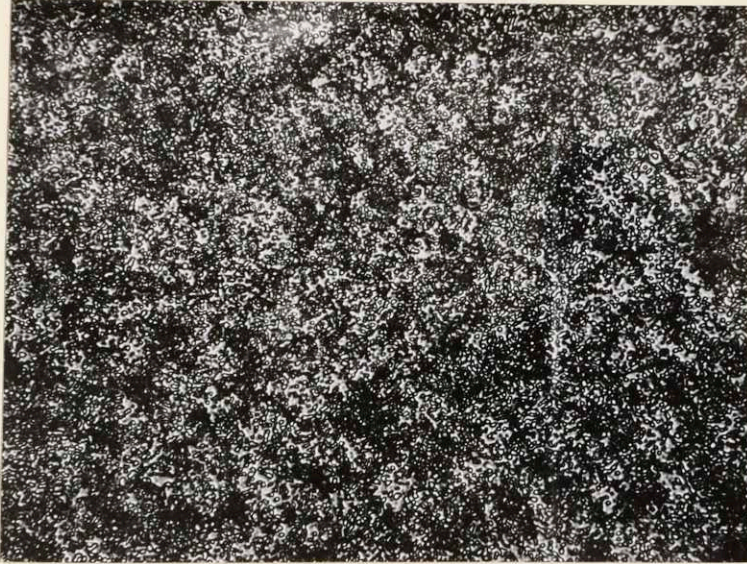


FIGURE 12

MICROSTRUCTURE OF ANNEALED S.A.E. 52,100

500 X
Nital Etch

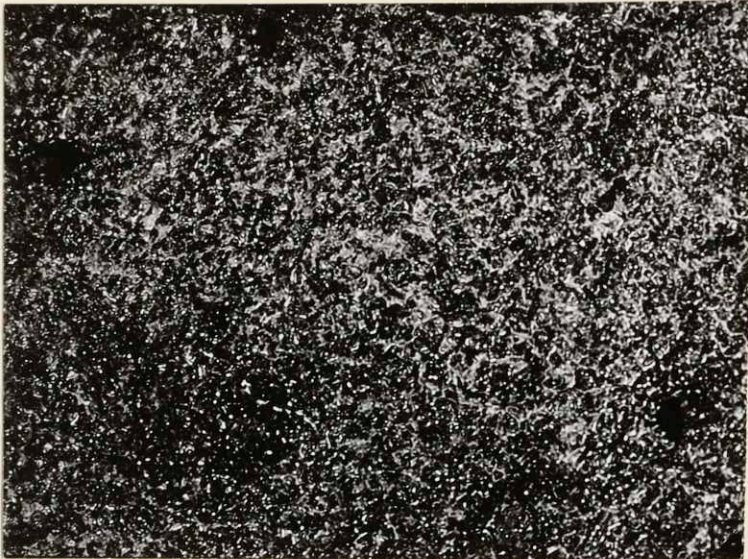


FIGURE 13

MICROSTRUCTURE OF OIL-QUENCHED S.A.E. 52,100

500 X
Nital Etch

ROCKWELL C HARDNESS
VS.
DRAWING TEMPERATURE

FOR S.A.E. 52100 $\frac{1}{2} \times \frac{1}{2} \times 3$ INCHES

Quenched in Oil From 1550° Degrees
Fahrenheit
Held 1 Hour at Tempering Temperature

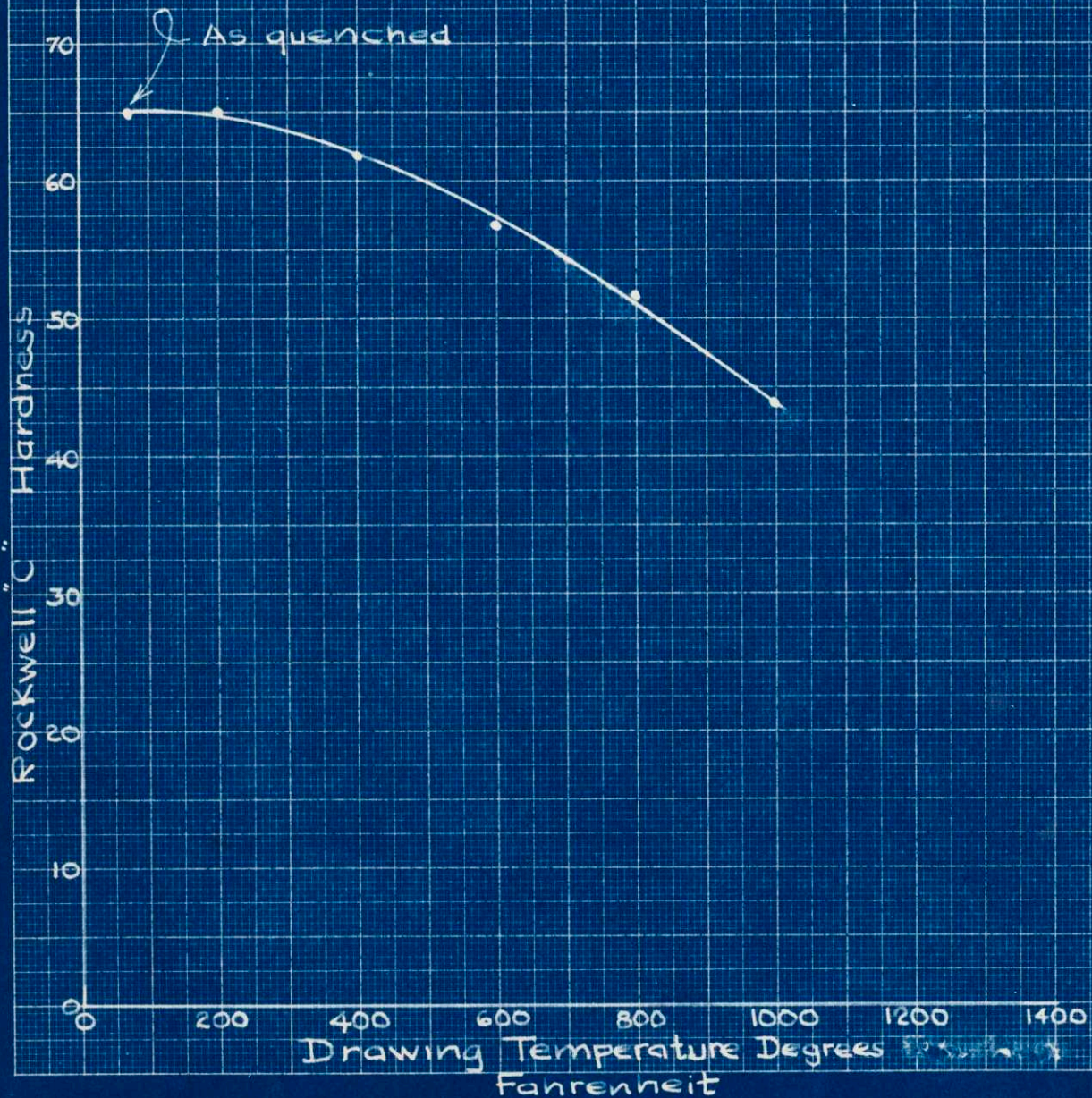


FIGURE 1A

Chart Speeds: 25 millimeters per second

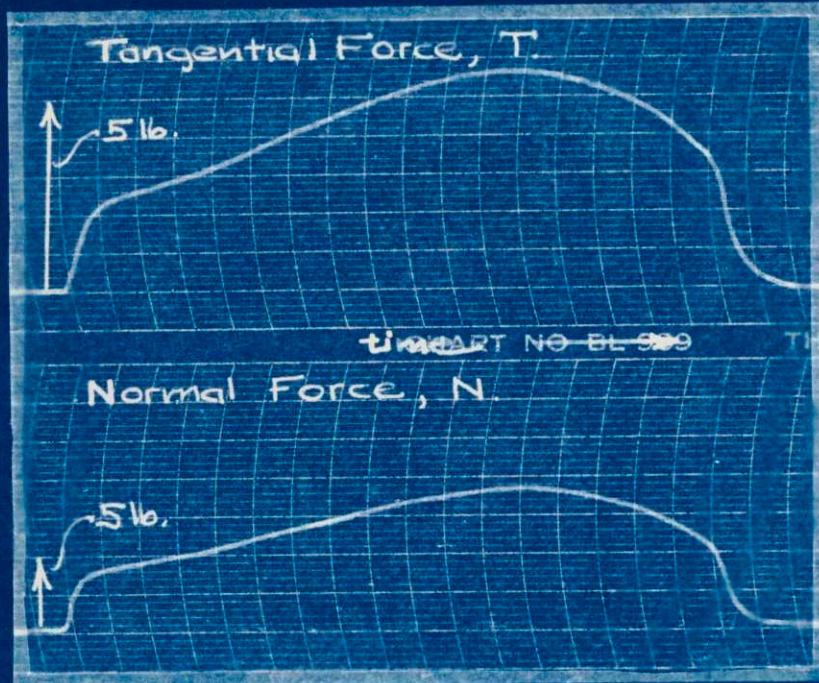


FIGURE 15

BRUSH CHART FOR HORIZONTAL WORK

Work Surface: $3 \times \frac{1}{2}$ inch, dry
Work: Annealed 52,100
Wheel: 32A46-HBVB, $8 \times \frac{3}{4}$ inch, 3000 rpm.
Table Speed: 4 feet per minute
Down Feed: 0.001" inch from work level

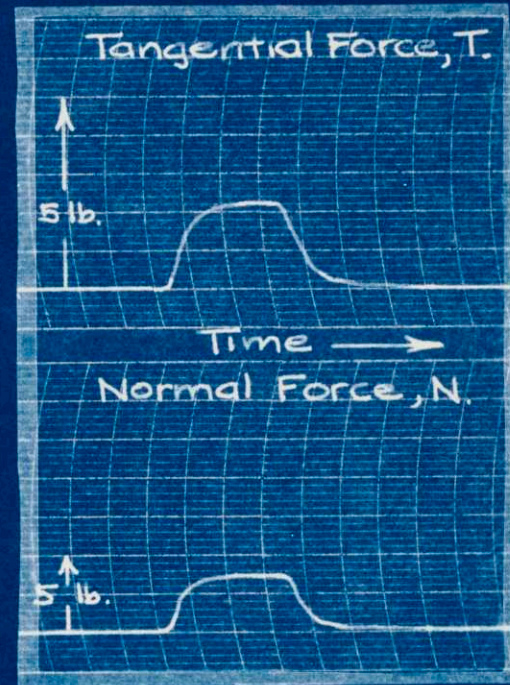


FIGURE 16

CHART FOR VERTICAL WORK

(Conditions same as Fig 15 except work surface $\frac{1}{2} \times \frac{1}{2}$ inch.)

GRAPH OF NORMAL, N, AND TANGENTIAL, T, FORCES FOR SPEC-
 IFIED SUCCESSIVE GRINDING WHEEL PASSES
 ALSO ACTUAL CUT DEPTH REMOVED PER PASS

The forces and cut depth approach a limit for successive equal feeds because of elasticity in the grinding system

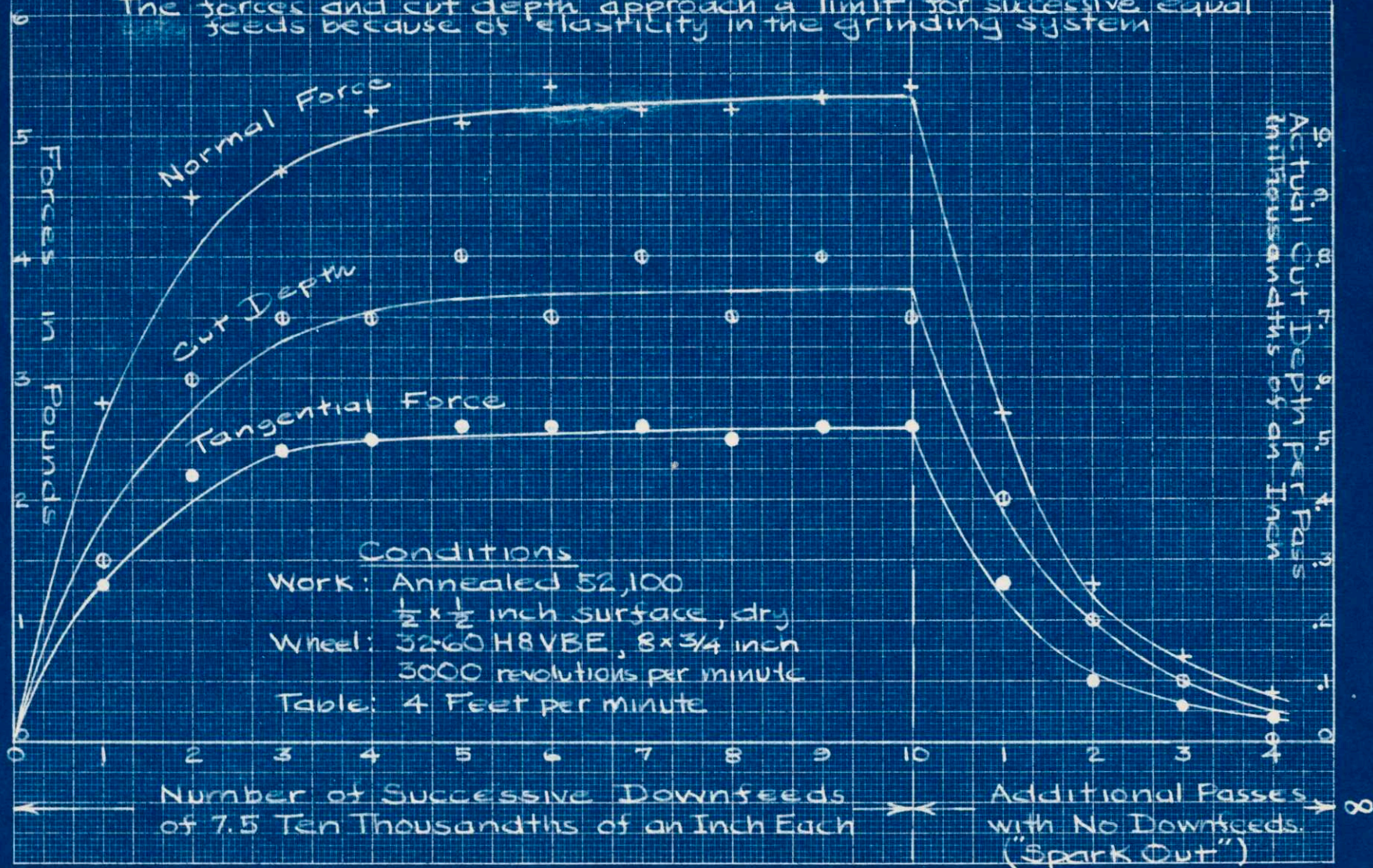


FIGURE 17.

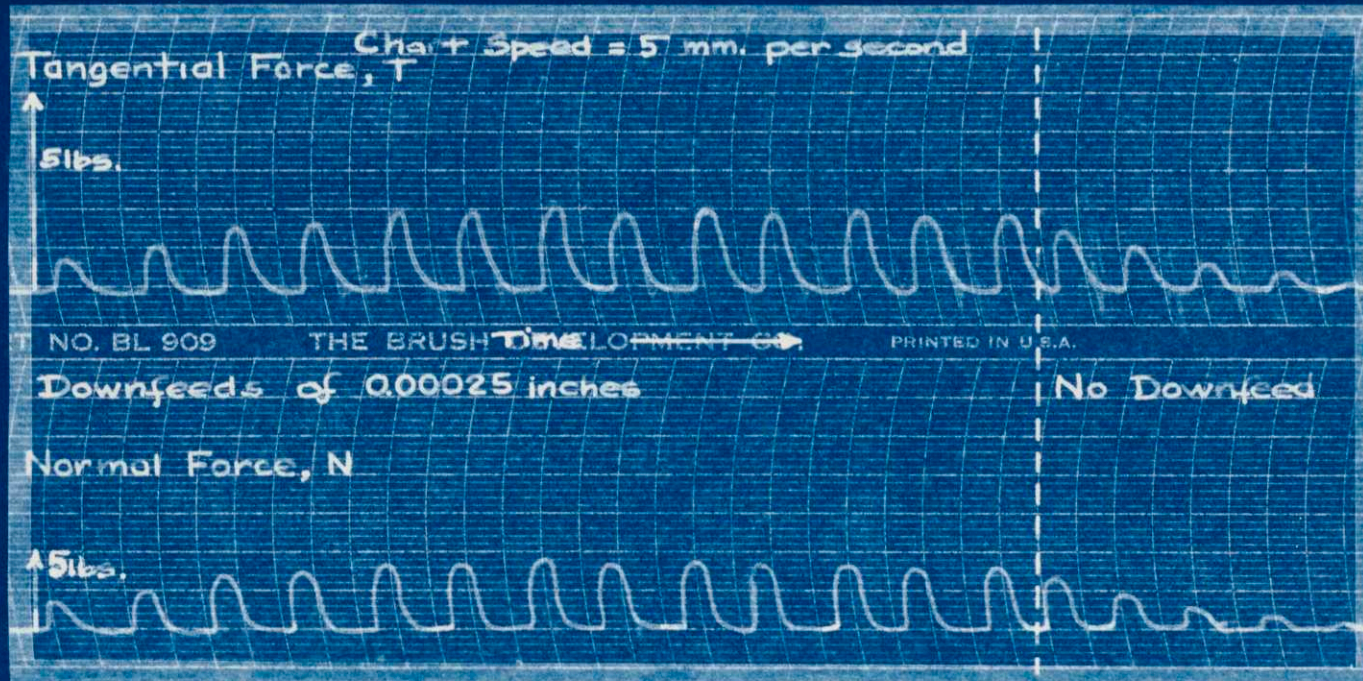


FIGURE 18.
TEST RUN SHOWING FORCES APPROACHING LIMITING VALUES

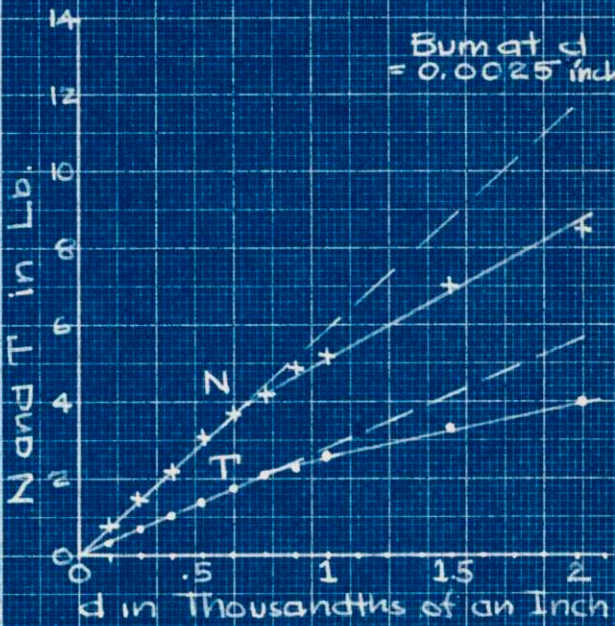
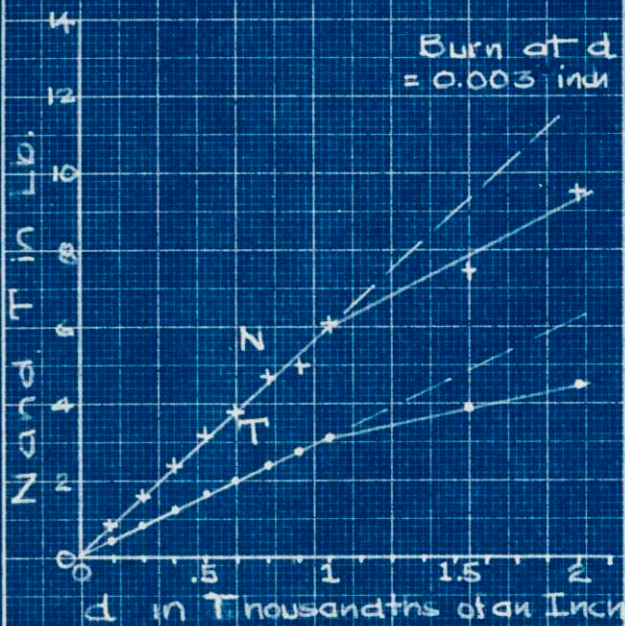
Work: Annealed 52,100
 Work Surface: $\frac{1}{2} \times \frac{1}{2}$ inch
 Wheel: 37C36JV
 Wheel Speed: 3000 revolutions per minute
 Table Speed: 4 feet per minute
 Cut Depth: 0.00025 inches at limit

NORMAL, N, AND TANGENTIAL, T, GRINDING FORCES VS. CUT DEPTH, d.

Work: Annealed 52,100; $\frac{1}{2} \times \frac{1}{2}$ inch surface; dry. Table: 4 Feet
 Wheel: 3000 rpm. for $8 \times \frac{3}{4}$ inch (specified below). Minute

36, Alundum (32A36HBVBE)

46, Alundum (32A46HBVBE)



60, Alundum (32A60HBVBE)

Silicon Carbide (37C36JV)

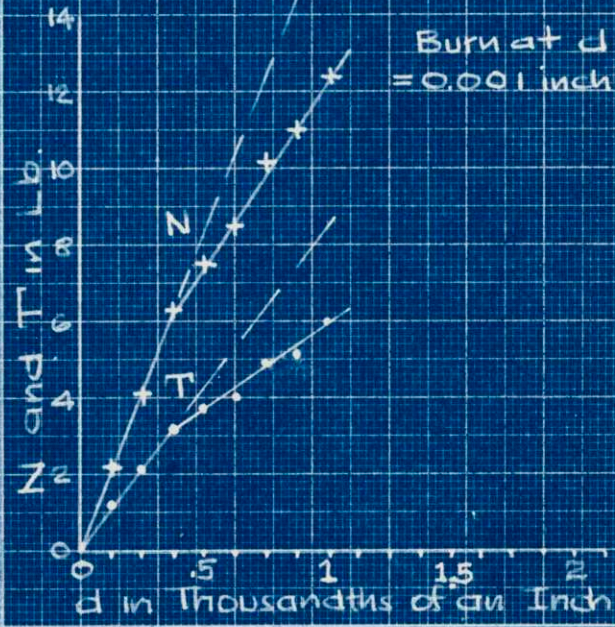
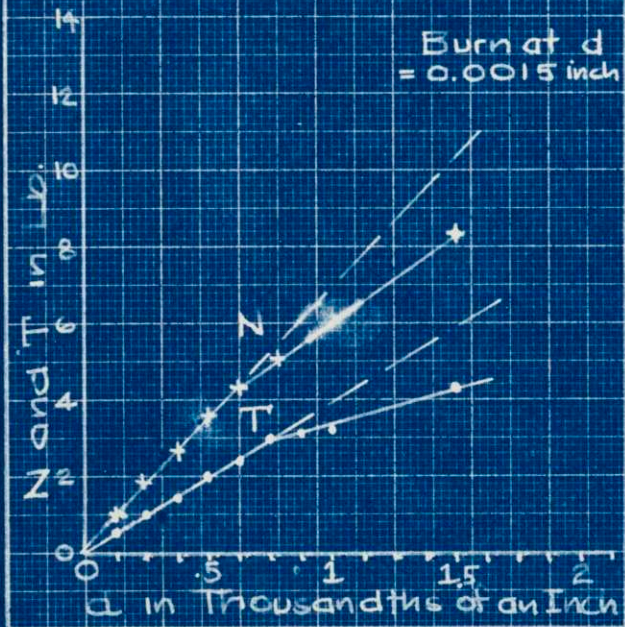
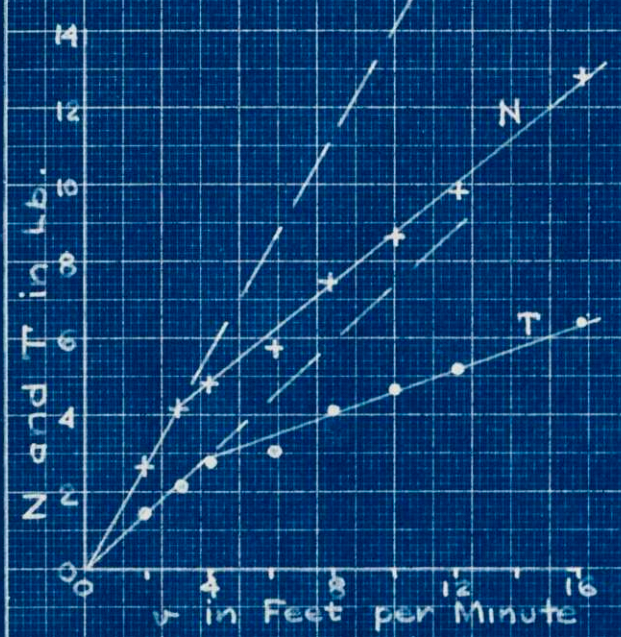


FIGURE 19.

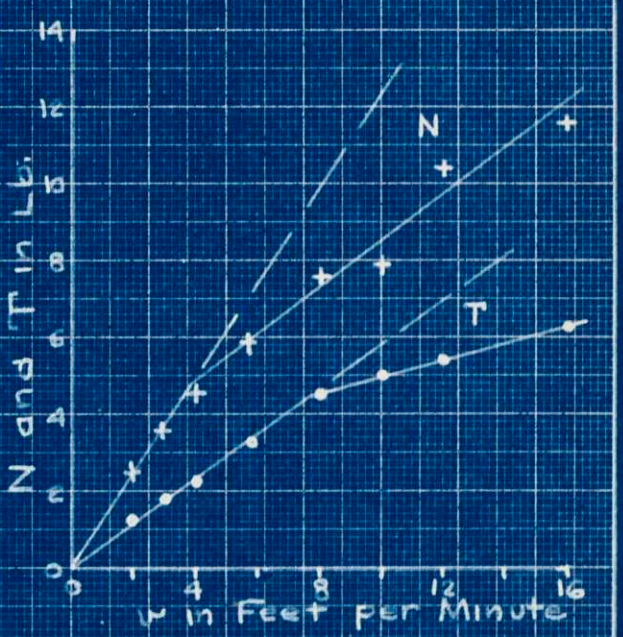
NORMAL, N, AND TANGENTIAL, T, GRINDING FORCES VS. TABLE SPEED, v , FOR FOUR SPECIFIED WHEELS

WORK: Annealed 52,100; $\frac{1}{2} \times \frac{1}{2}$ inch surface cut; See Wheel Spag: 3000 rpm for $8 \times \frac{3}{4}$ inch wheel below

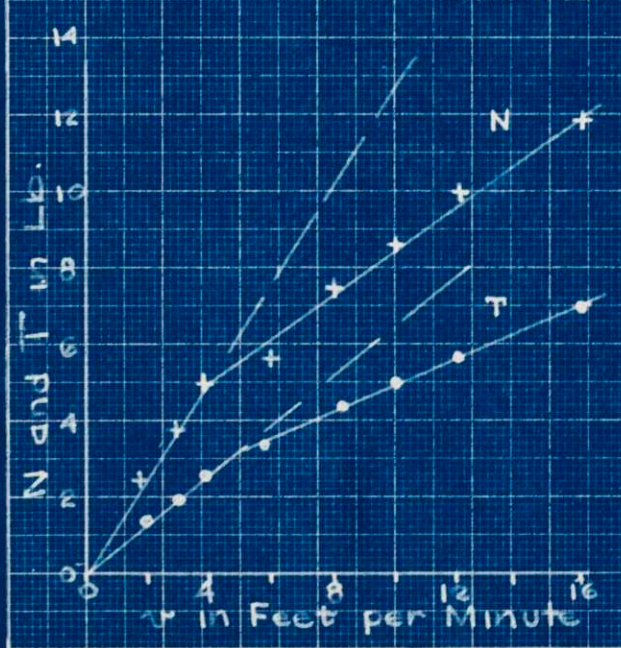
36, Alundum (32A36-H8VBE)
Cut Depth, $d = .00075$ inches



46, Alundum (32A46H8VBE)
Cut Depth, $d = 0.00075$ inches



60, Alundum (32A60-H8VBE)
Cut Depth, $d = 0.00075$ inches



36, Silicon Carbide (37C36UV)
Cut Depth, $d = 0.0025$ inches

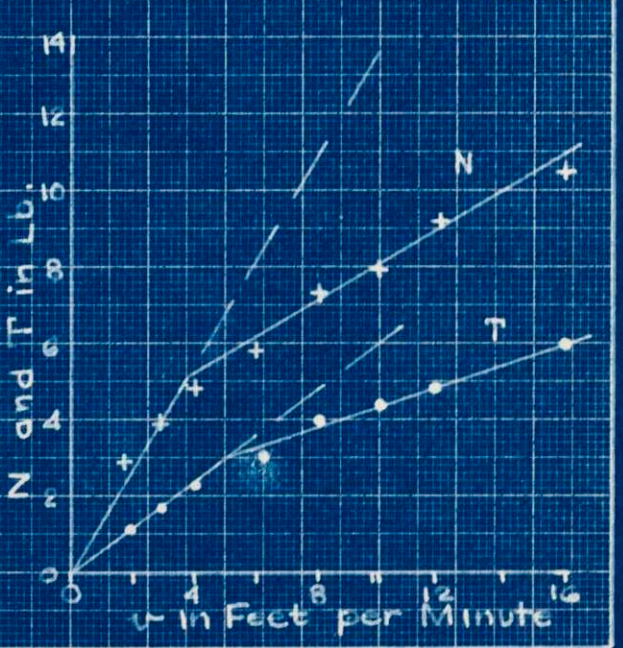


FIGURE 20

NORMAL, N, AND TANGENTIAL, T, GRINDING FORCES VS. THE INVERSE OF THE WHEEL SPEED, $\frac{1}{n}$

Work: Annealed 52,100 $\frac{1}{2} \times \frac{1}{2}$ inch surface

Wheels: $8 \times \frac{3}{4}$ inches specified below.

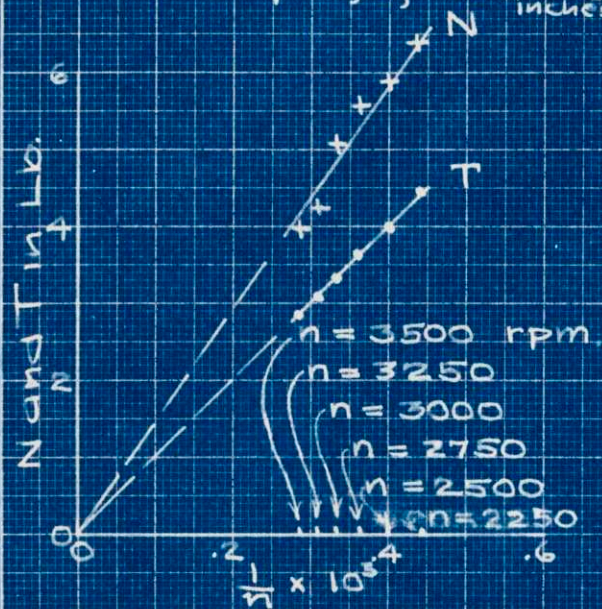
Table Speed: 4 feet per minute.

Cut Depths: As specified below. (d)

Wheel Speeds: 2250, 2500, 2750, 3000, 3250, 3500 rpm

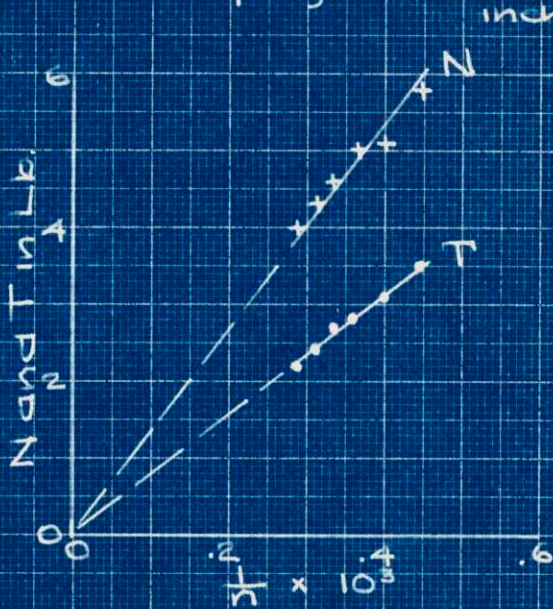
36, Alundum (32A36HVB)E

Cut Depth, $d = .00075$ inches



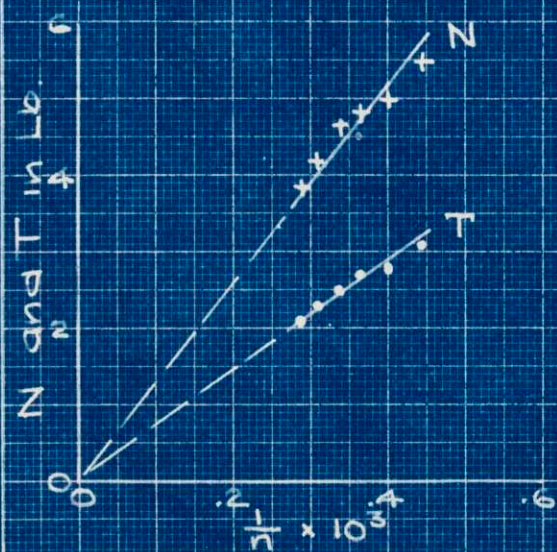
46, Alundum (32A46HBVBE)

Cut Depth, $d = .00075$ inches



60, Alundum (32A60HBVBE)

Cut Depth, $d = .00075$ inches



36, Silicon Carbide (37C36IV)

Cut Depth, $d = .00025$ inches

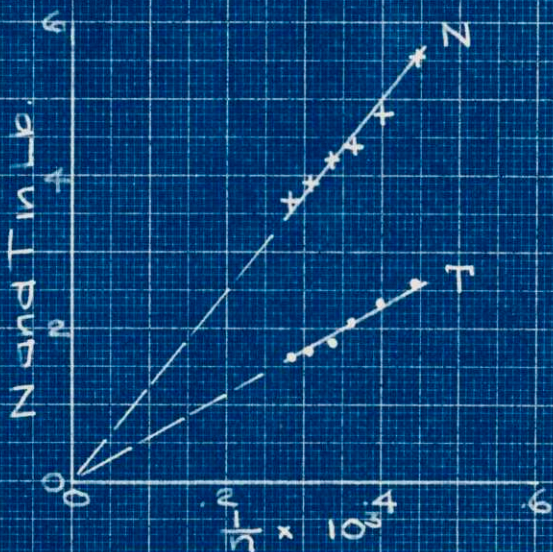
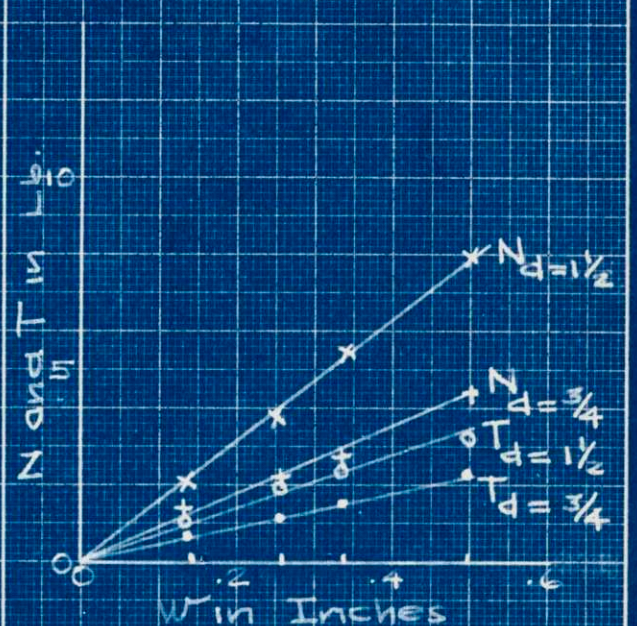
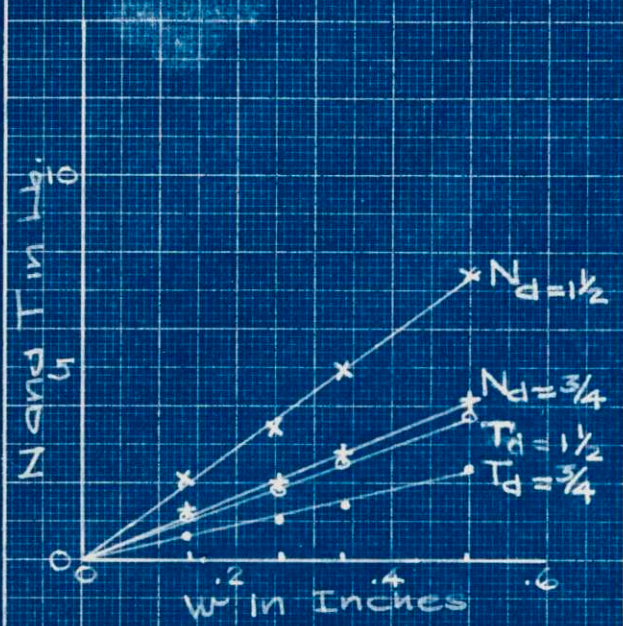


FIGURE 21

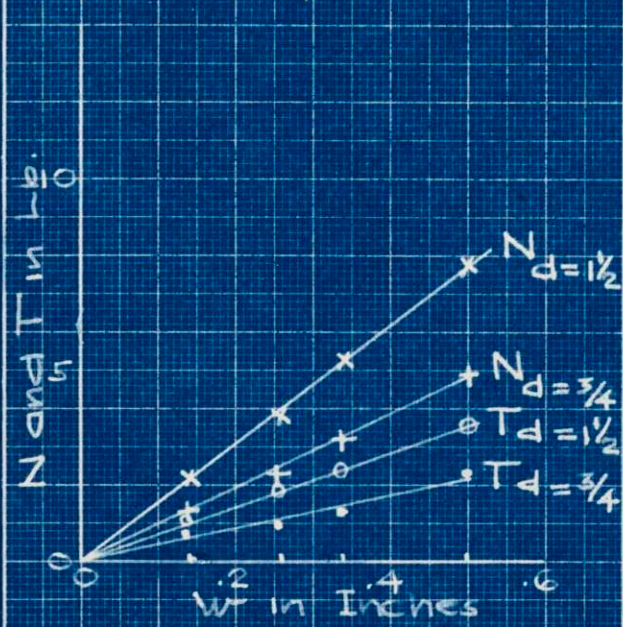
NORMAL, N, AND TANGENTIAL, T GRINDING FORCES VS. WIDTH, W, OF THE WORK

Work: Annealed 52,100, $\frac{1}{2}$ along table
 Wheels: $8 \times \frac{3}{4}$ inch, specified below 3000 rpm.
 Table Speed: 4 feet per minute
 Cut Depths: Two for each wheel, (see sub-script, d, on force symbols N & T, i.e. $N_d = 1\frac{1}{2}$ means $1\frac{1}{2}$ thousandths inches)

36, Alundum (32A36H8VBE) 46, Alundum (32A46H8VBE)



60, Alundum (32A60H8VBE)



36, Silicon Carbide (37C36J1)

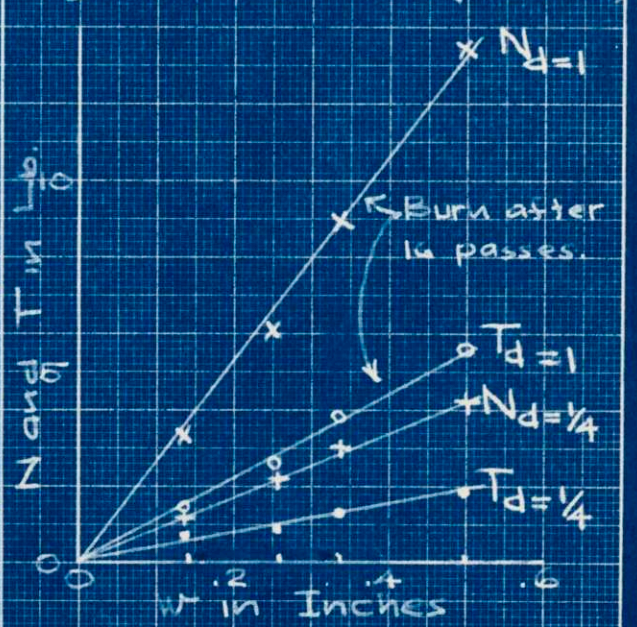
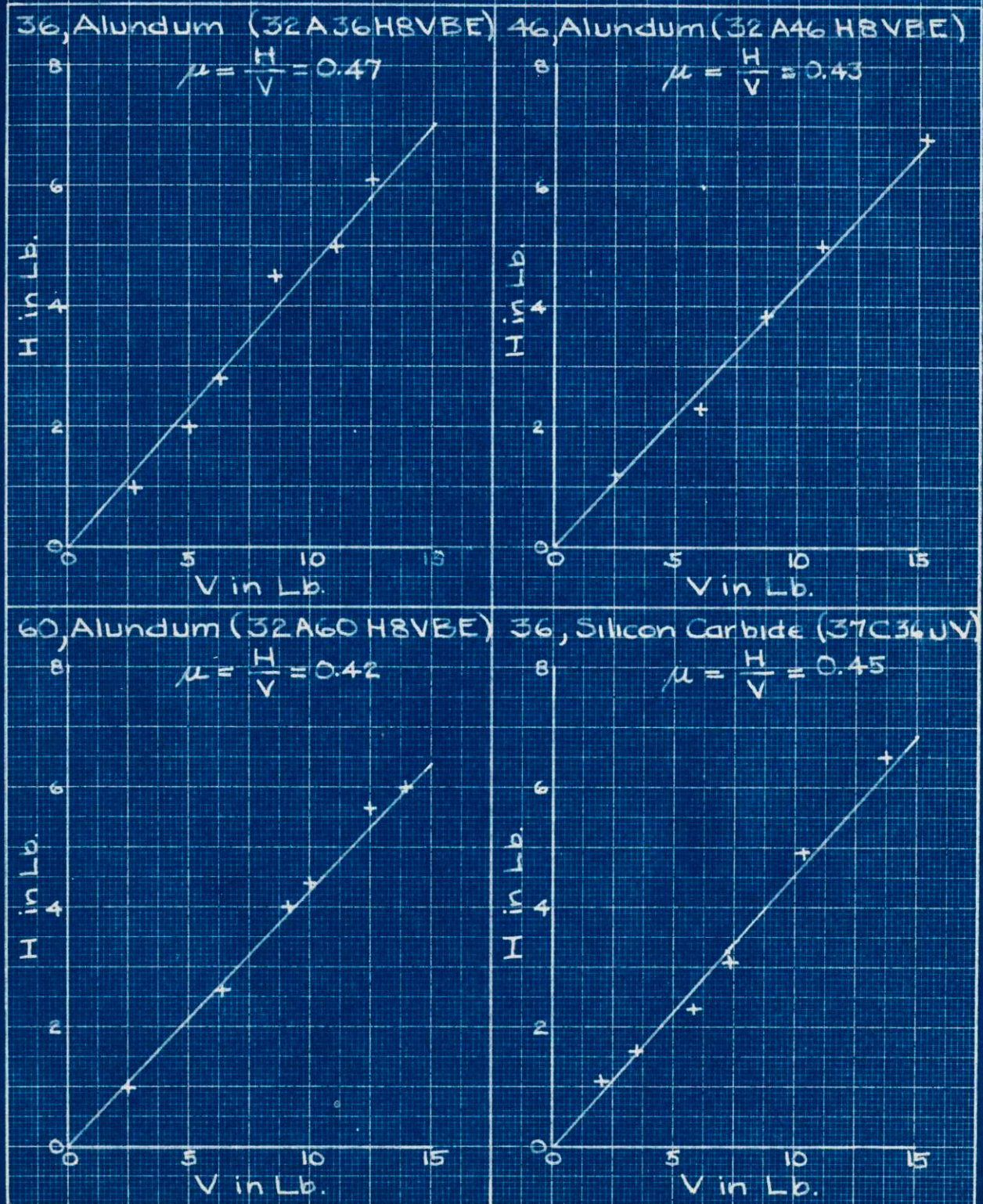


FIGURE 22

HORIZONTAL, H, vs. VERTICAL, V, FRICTION FORCES
FOR
ANNEALED 52,100 AGAINST FOUR SPECIFIED WHEELS



(Note: Wheel fixed, work moved by table)

FIGURE 23

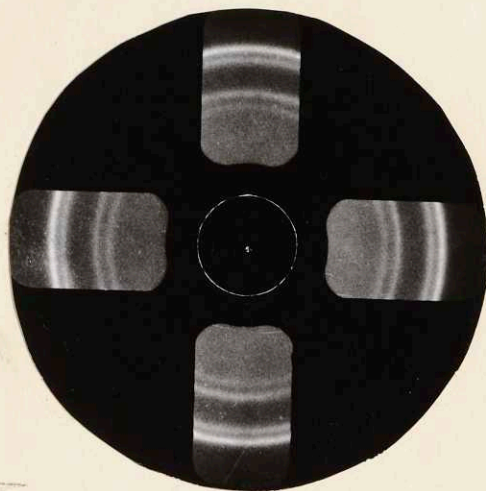


FIGURE 24

X-RAY DIFFRACTION RINGS FOR
ANNEALED SPECIMEN

Rings reading toward center as follows:

α_1 222 Tungsten (reference powder)

α_2 222 Tungsten " "

α_1 310 Iron

α_2 310 Iron

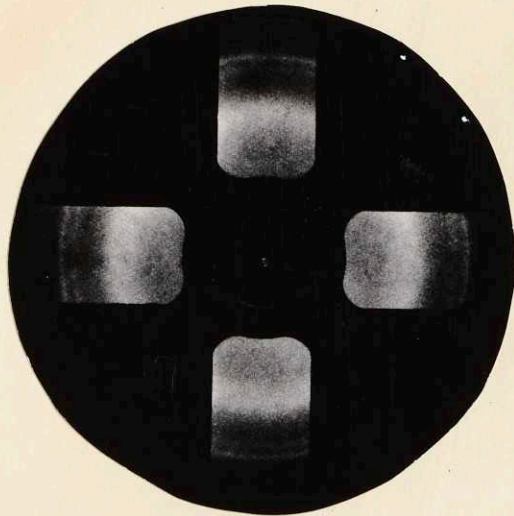


FIGURE 25

DIFFRACTION RINGS FOR
GROUND SURFACE

Cut Depth: 0.00025 inches

Etch Depth: 0

Fe α : Unresolved

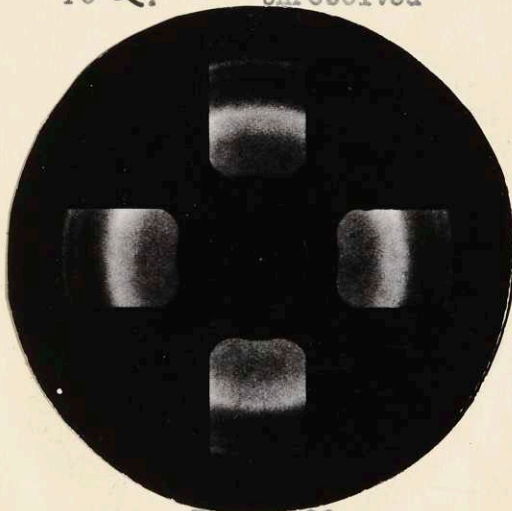


Figure 26

DIFFRACTION RINGS FOR
GROUND SURFACE

Cut Depth: 0.00025 inches

Etch Depth: 0.00020 inches

Fe α : Faintly resolved

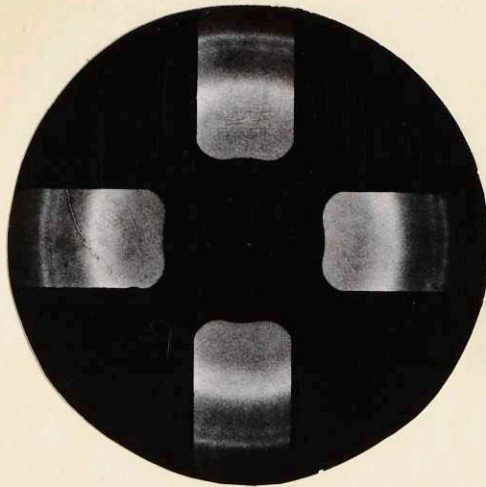


FIGURE 27

DIFFRACTION RINGS FOR
GROUND SURFACE

Cut Depth: 0.00050 inches
Etch Depth: 0.00020 inches
Fe α : Unresolved

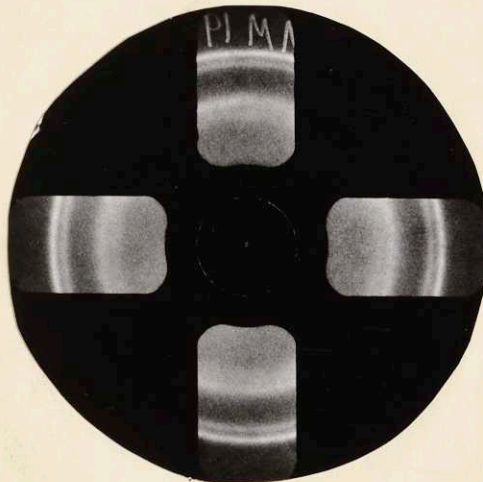


FIGURE 28

DIFFRACTION RINGS FOR
GROUND SURFACE

Cut Depth: 0.00050
Etch Depth: 0.00040
Fe α : Faintly resolved.

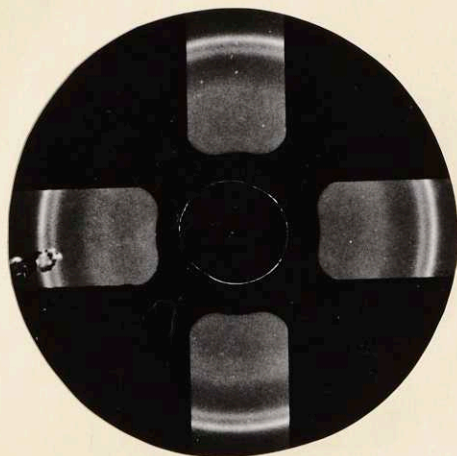


FIGURE 29

DIFFRACTION RINGS

FOR GROUND SURFACE

Cut Depth: 0.00100 inches

Etch Depth: 0.00040 inches

Fe α : Unresolved

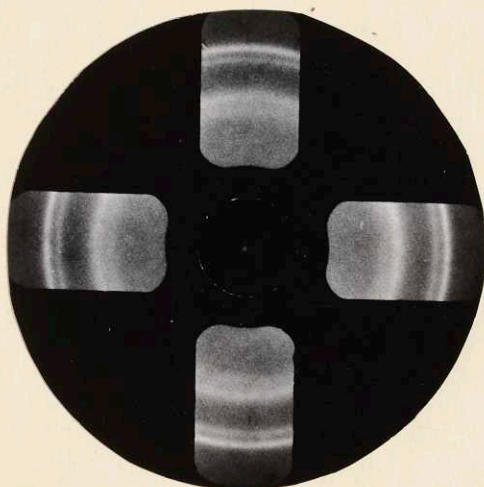


FIGURE 30

DIFFRACTION RINGS

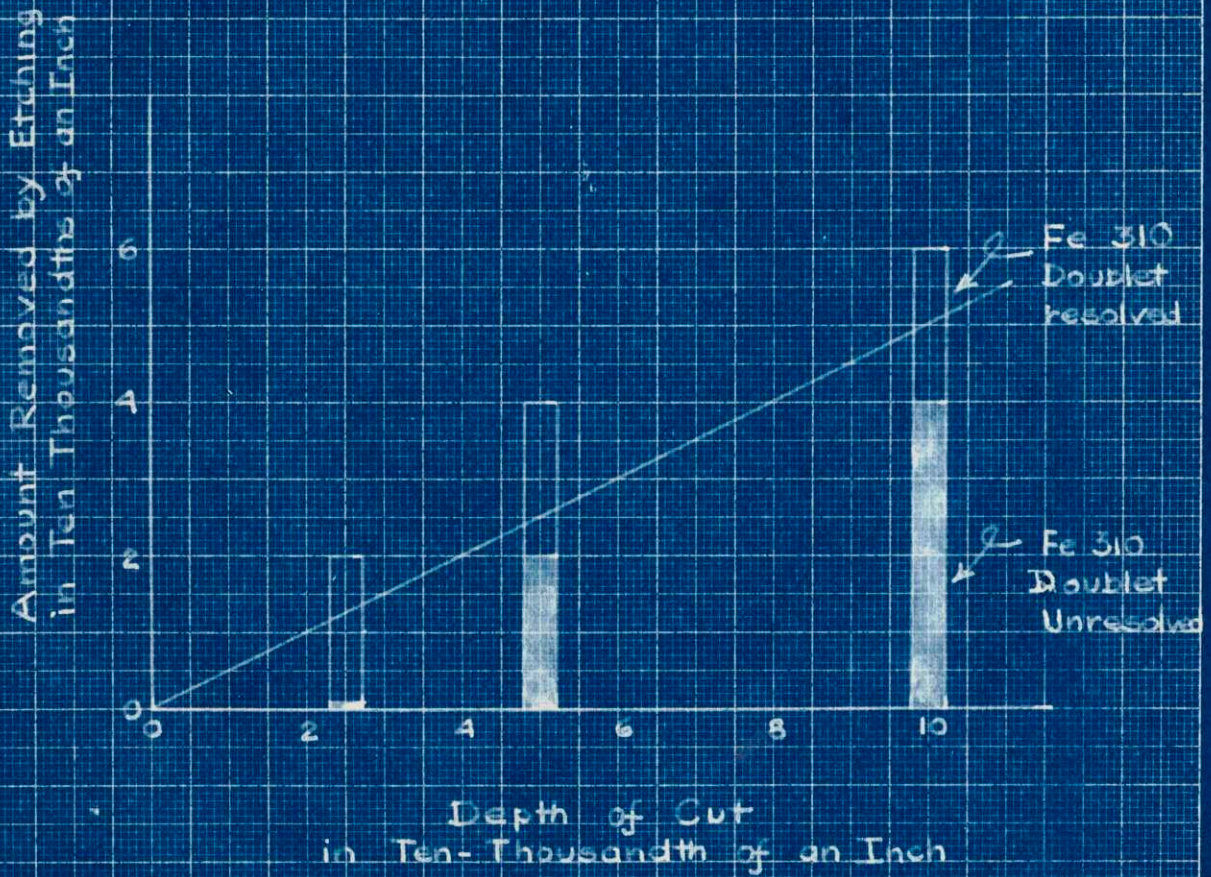
FOR GROUND SURFACE

Cut Depth: 0.00100 inches

Etch Depth: 0.00060 inches

Fe α : Resolved

FIGURE 31
DEPTH OF COLD-WORKING
AS INDICATED BY RESOLUTION
OF THE Fe 310 DOUBLET



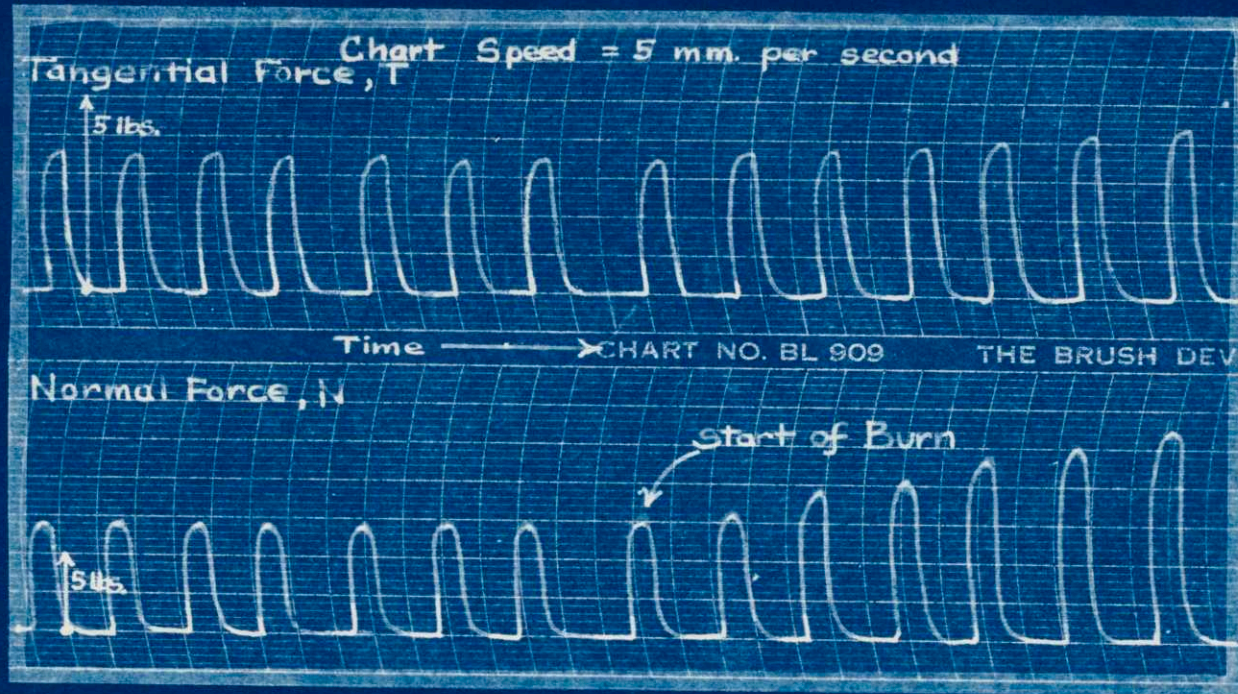


FIGURE 32.
BRUSH CHART SHOWING FORCES FOR SURFACE BURN

Work: Annealed 52,100
 Work Surface: $\frac{1}{2} \times \frac{1}{2}$ inch
 Wheel: 32A60-H8VBE
 Wheel Speed: 3000 revolutions per minute
 Table Speed: 4 feet per minute
 Cut Depth: 0.0010 inches

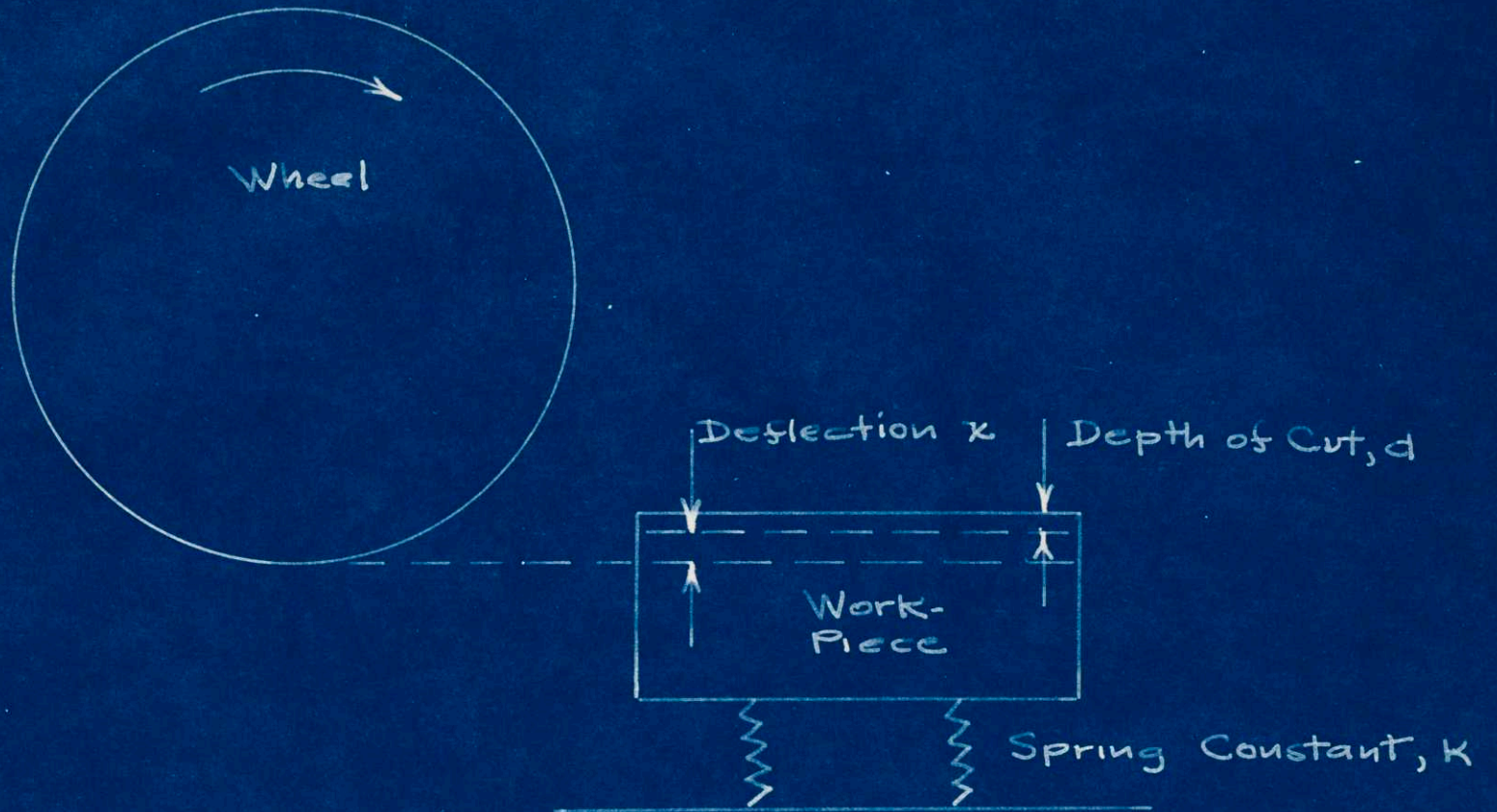


DIAGRAM FOR ELASTIC ANALYSIS

FIGURE 33

ENERGY PER UNIT VOLUME OF CHIP, E/V
 vs.
 POWER FROM WHEEL, P

$$E/V = \frac{2\pi r \times T \times n}{v \times W \times d}$$

Where: r = radius of wheel
 T = Tangential Force
 n = Wheel Speed (for 32A46-HBYBE)
 v = Table Speed
 d = Cut Depth
 W = Work Width

Point	d inches $\times 10^4$	v inches minute	n rpm.	T L_6
1	7.5	48	3000	2.2
2	3.75	48	3000	1.4
3	5	26	2250	3.1
4	1	36	2750	2.3
5	2.5	36	2750	.75
6	5	36	3250	1.2
7	1	56	3250	1.2
8	5	180	3250	2.8
9	1.25	48	5000	.4

} Points on Graph

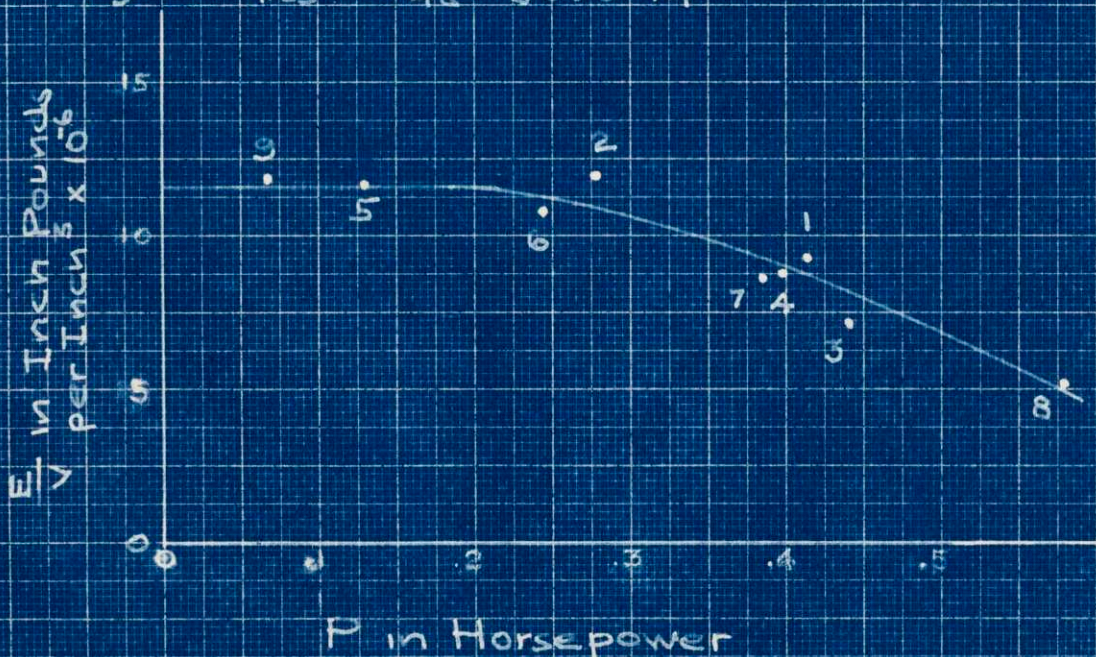


FIGURE 34
 GENERALIZED PLOT OF GRINDING DATA